Bridge Scour Manual

Supplement to Austroads Guide to Bridge Technology Part 8, Chapter 5: Bridge Scour (2018)

January 2019

Queensland Government

Copyright

Licence

CC BY licence summary statement

Translating and interpreting assistance

The Queensland Government is committed to providing accessible services to Queenslanders from all cultural and linguistic backgrounds. If you have difficulty understanding this publication and need a translator, please call the Translating and Interpreting Service (TIS National) on 13 14 50 and ask them to telephone the Queensland Department of Transport and Main Roads on 13 74 68.

Disclaimer

Feedback

Please send your feedback regarding this document to: tmr.techdocs@tmr.qld.gov.au

About this document

The second edition of the *Bridge Scour Manual*, sets out a multi-disciplinary approach to the estimation of the depth and extent of scour required for design of waterway bridges. It is a guide to those involved in the planning, design, operation and maintenance of bridges spanning waterways.

This manual has been technically reviewed by Professor Bruce Melville from the Department of Civil and Environmental Engineering at The University of Auckland, New Zealand. Transport and Main Roads acknowledges his contribution to this manual update.

This manual represents the policy of the Department of Transport and Main Roads with respect to the planning, design, operation and maintenance of scour in bridges and must be applied on all road infrastructure projects for which the department is responsible. As such, the manual applies equally to all personnel, departmental or not, that are involved in the bridge scour aspects of departmental projects This manual is to be used by appropriately qualified and experienced personnel.

In the interest of national uniformity and eliminating duplication of material, this second edition of the *Bridge Scour Manual* has been edited to formally cross-reference to the *Guide to Bridge Technology Part 8: Hydraulic Design of Waterway Structures, Chapter 5: Bridge Scour* (herein referenced as Austroads, 2018). In addition, the department has adopted the *Australian Rainfall and Runoff* (ARR, 2016) nomenclature to describe the occurrence of flood events.

Where such references are made, the relevant section in the *Austroads Guide to Bridge Technology, Part 8: A Guide to the Waterway Design for Structures, Chapter 5: Bridge Scour* will be quoted as being accepted or accepted with amendments and the corresponding content will have been removed from this *Bridge Scour Manual*. Where a section of the *Austroads Guide to Bridge Technology* is accepted with amendments, the amendments can take one of two forms:

Addition(s): where the *Bridge Scour Manual* provides additional guidance specific to departmental policies and practices.

Difference(s): where the *Bridge Scour Manual* provides guidance specific to departmental policies and practices, to be used instead of that contained within the quoted sections of *Austroads Guide to Bridge Technology*.

The following table summarises the relationship between the *Austroads Guide to Bridge Technology, Part 8: A Guide to the Waterway Design for Structures, Chapter 5: Bridge Scour* and this document.

Applicability	Meaning
Accepted	The Austroads guide section is accepted as is.
Accepted with amendments	Part or all of the section or clause has been accepted with additions, deletions or differences.
New content	There is no equivalent section within the Austroads guide.
Not accepted	The Austroads guide section is not accepted.

Relationship table

Chapter	Section	Description	Applicability
5.1	Introduction		Accepted with Amendments
5.2	**Scour Characteristics**		
	5.2.1	General	Accepted
	5.2.2	Types of Scour	Accepted with Amendments
	5.2.3	Factors Affecting Scour	Accepted with Amendments
	5.2.4	Clear-Water and Live-Bed Scour	Accepted with Amendments
	5.2.5	Aggradation and Degradation	Accepted with Amendments
	5.2.6	Scour Due to River Morphology	Accepted with Amendments
	5.2.7	Contraction Scour	Accepted with Amendments
	5.2.8	Local Scour	Accepted with Amendments
5.3	**Bridge Scour Design and Evaluation**		
	5.3.1	General	Accepted with Amendments
	5.3.2	New Bridges	Accepted with Amendments
	5.3.3	Existing Bridges	Accepted with Amendments
	5.3.4	Design Procedures for Abutment Protection	Accepted
	5.3.5	Foundation Design to Resist Scour	Accepted
	5.3.6	Evaluation of Foundation Design for ULS Scour	Accepted
	5.3.7	Scour Related to Construction	Accepted with Amendments
5.4	**Methods of Estimating Scour**		
	5.4.1	General	Accepted with Amendments
	5.4.2	Design Approach	Accepted with Amendments
	5.4.3	Live-bed Contraction Scour	Accepted with Amendments
	5.4.4	Clear-water Contraction Scour	Accepted
	5.4.5	Contraction Scour with Backwater	Accepted
	5.4.6	Contraction Scour in Cohesive Materials	Accepted with Amendments
	5.4.7	Contraction Scour in Erodible Rock	Accepted with Amendments
	5.4.8	Mean Velocity Method	Accepted with Amendments
	5.4.9	Scour at Abutments	Accepted with Amendments
	5.4.10	Local Scour at Piers	Accepted with Amendments

Chapter	Section	Description	Applicability
	5.4.11	Pressure Flow Scour	Accepted with Amendments
	5.4.12	Worked Examples	Accepted with Amendments
5.5	**Scour Countermeasures**		
	5.5.1	Introduction	Accepted with Amendments
	5.5.2	Countermeasure Groups and Characteristics	Accepted with Amendments
	5.5.3	Considerations for Selecting Countermeasures	Accepted with Amendments
	5.5.4	Design of Countermeasures	Accepted with Amendments
5.6	**Monitoring Bridges for Scour**		
	5.6.1	Sonar Scour Monitor	Accepted with Amendments
	5.6.2	Magnetic Sliding Collar monitor	Accepted with Amendments
	5.6.3	Float-out Devices	Accepted with Amendments
	5.6.4	Sounding Rods	Accepted with Amendments
	5.6.5	Time Domain Reflectometry (TDR)	Accepted
	5.6.6	Ground-Penetrating Radar (GPR)	Accepted
	5.6.7	Tiltmeter Arrays	Accepted
	5.6.8	Operational Considerations	Accepted with Amendments

Contents

Tables

Figures

5 Bridge Scour

5.1 Introduction

Addition

Melville and Coleman (2000), contains a comprehensive review of scour processes at bridges.

Melville and Coleman (2000) and Kirby et al. (2015) are additional reference documents that have been relied upon during the preparation of the present manual update.

5.2 Scour characteristics

5.2.1 General

5.2.2 Types of scour

Addition

Aggradation, degradation and river morphology scour are often referred as to General Scour, this type of scour occurs irrespective of the bridge and can occur over short or long term. Contraction and local scour are jointly referred to as localised scour, this type of scour is solely caused by bridges.
Table 5.2.2 presents a classification of the types of scour occurring at bridges.

Table 5.2.2 – Types of scour at a bridge crossing

Total Scour			
General / Natural Scour		**Localised Scour**	
Long term	**Short term**	**Contraction Scour**	**Local Scour**
Aggradation / degradation	Bend scour		Pier scour
Channel migration	Confluence scour		Abutment scour
	Bed form migration (sediment wave)		

Adapted from (Melville and Coleman 2000)

Total scour depth at a bridge is the sum of:

- Natural / general scour
- Contraction scour if applicable, and
- Local scour at piers and abutments.

All factors contributing to scour are subject to a significant degree of uncertainty; as such long-term predictions are difficult, as information available on major floods might be limited and the flow conditions may be altered by changes in catchment or climate.

5.2.3 Factors affecting scour

Addition

Table 5.2.3 summarises hydrologic, geomorphic, flood flow, bed sediment and bridge geometry factors that can influence scour processes at bridges.

Key processes and drivers of general/natural scour and stream rehabilitation are discussed in detail within the Queensland Stream Management guidelines and the wetland management resources in Queensland website (https://wetlandinfo.des.qld.gov.au/wetlands/).

Table 5.2.3 – Factors influencing bridge scour

		General Scour	Localised Scour
Hydrologic	Rainfall	x	
	Topography / slope	x	
	Size	x	
	Shape	x	
	Vegetation	x	
	Type of Soil / erodibility	x	
Geomorphic	Floodplain configuration	x	
	Stream width and variability	x	
	Cross- sectional shape	x	
	Channel slope	x	
	Degree of incision	x	
	Hydraulic controls	x	
	Sinuosity	x	
	Presence of braids / anabranches and bars	x	
	Bank materials	x	
	Bank slope stability	x	
	Vegetal cover	x	
Flood Flows	Flow rate	x	x
	Flood duration	x	x
	Velocity	x	x
	Lateral velocity distribution	x	x
	Secondary currents	x	x
	Sediment Transport rate and form	x	x
	Debris load	x	x
Bed Sediment	median size (d_{50})	x	x
	non-uniformity (σ_g)	x	x
	Cohesion (C)	x	x
	Vertical stratification	x	x
	Areal distribution	x	x
	Erodibility of material	x	x
	Presence of bedrock	x	x
Bridge Geometry	Contraction at Bridge opening		x
	Submergence of superstructure		x
	Location with respect to channel bends		x
	Type of bridge piers/abutments		x
	Position of piers/abutments in channel		x
	Shape of piers/abutments		x
	Size and length of piers/abutments		x
	Skewness of piers/abutments		x
	Revetments, retards, spurs, guidebanks		x
	Bridge modifications		x

Adapted from (Melville and Coleman 2000).

5.2.4 Clear-water and live-bed scour

Difference

Figure 5.3 reference is incorrect, source is Arneson et al. (2012).

5.2.5 Aggradation and degradation

Addition

Aggradation and degradation are the processes of long-term deposition and erosion of bed material in rivers (Kirby et al. 2015), these processes occurring progressively over time. They are often encompassed within the so-called general or natural scour processes.

Aggradation and degradation refer to the building up and lowering of bed levels in rivers respectively. Aggradation occurs when the sediment loads in the river exceed its sediment transport capacity, conversely, degradation occurs when the sediment loads in the river are lower than its sediment transport capacity. Stable regime (equilibrium) conditions in streams can be disturbed by factors listed in Table 5.2.3.

5.2.6 Scour due to river morphology

Addition

Scour processes in a stream are influenced by its geomorphic characteristics (that is, type and form) and its sediment properties. The typology and appearance of a stream can provide information on its likely geomorphic features, sediment characteristics and processes and can help predicting river behaviour.

River typologies in Northern Australia are documented in Saynor et al. (2008). Most of the cited typologies found in Queensland can be grouped into three main categories:

- **Upstream bedrock channels** – they usually have steep or moderate slopes, are incised in highly resistant lithologies, have essentially no-floodplain and have low sediment loads.
- **Alluvial rivers / floodplains** – are usually found in middle sections of the catchment, have gentle or flat slopes and are characterised by alluvial bed material with riparian vegetation along banks and floodplains; they can be ephemeral, intermittent or perennial and have large sediment loads usually influenced by anthropogenic activities. This class includes the most common road-crossed streams within Queensland (meandering rivers, braided rivers with anabranches, wandering channels and non-channelized river floodplains). For example, 77% of the streams in the Flinders River Catchment in Northwestern Queensland are braided / anabranching (Saynor et al. 2008), and
- **Estuarine Rivers** – streams influenced by tidal movements located in the lower catchments and estuaries with presence of cohesive silt on top of alluvial bed material.

Figure 5.2.6(a) shows a relationship between channel type, hydraulic and sediment factors and relative instability. This classification might be useful to qualitatively assess the likelihood of natural / general scour processes within the stream and the potential influence of proposed structures on such processes.

Figure 5.2.6(a) – Interrelationship between channel type, hydraulic and sediment factors and relative stability (After Shen et al. 2001)

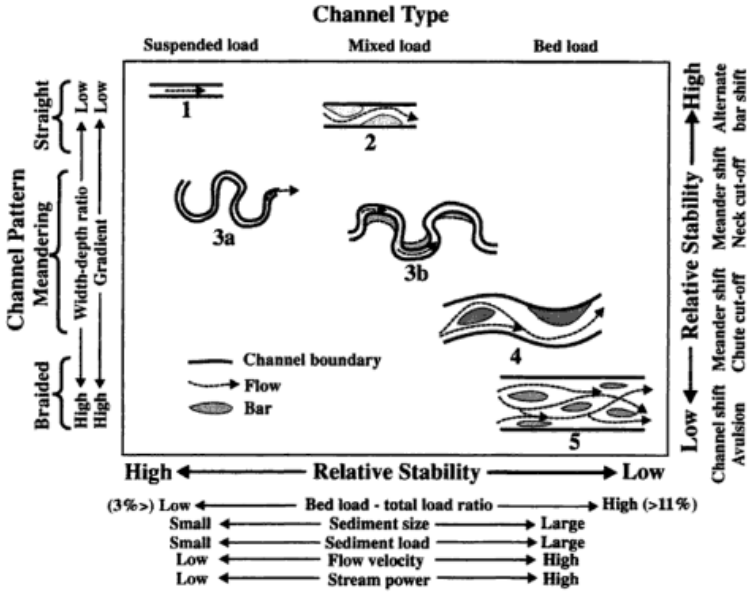

Braided channels are unstable and unpredictably prone to aggradation, degradation or lateral movement. Deepest scour in these channels can occur at the confluence of two or more major channels, downstream of a bar or island in the channel. These features can exacerbate scour at bridges. Anabranched streams separated by relatively stable islands are less prone to general scour than braided channels (Melville and Coleman 2000). Figure 5.2.6(b) shows an example of a road crossing over a Western Queensland braided river system during flood.

Figure 5.2.6(b) – Diamantina Developmental Road crossing of the Georgina River during flood, Bedourie - Boulia, Western Queensland

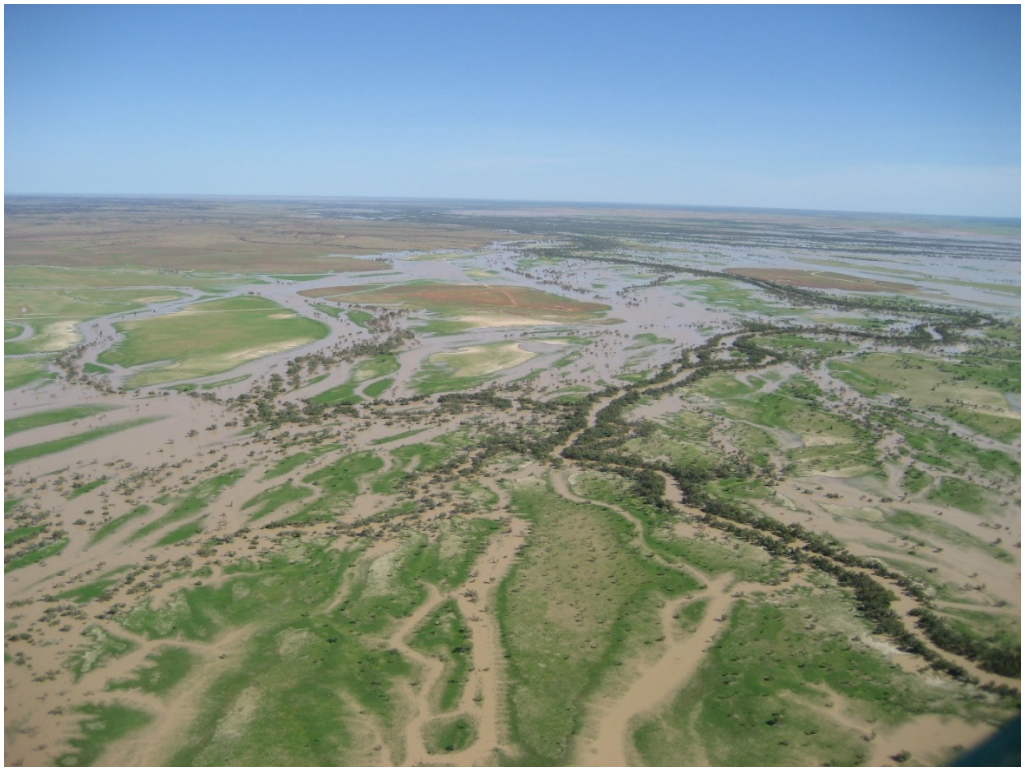

(Photo: Courtesy of Transport and Main Roads Central West District).

Other scour processes included within the natural / general scour definition are: channel migration, bend scour, confluence scour, lateral erosion and wave scour (refer to Table 5.2.2). These processes are briefly described in the following sections.

5.2.6.1 Channel migration

It can occur naturally or be caused by anthropogenic activity and is associated with aggradation / degradation processes. Migration of the stream or lowering of the deep-water channel (thalweg) changes local bed elevation and flow direction and can increase the risk of scour at bridge piers and abutments.

Potential of channel migration should be considered within bridge design. Alternatively, training works may be implemented to limit thalweg movement.

Figure 5.2.6.1 shows an example of bridge scour attributed to flood triggered channel migration upstream of the bridge.

Figure 5.2.6.1 – Bridge in South East Queensland

5.2.6.2 Bend scour

This process is directly attributed to flow curvature where velocity, shear stress and turbulent secondary currents increase towards the outside of the bend leading to larger scour at outer bends and deposition at inner bends (refer to Figure 5.2.6.2). Methods to evaluate bend scour are discussed in Section 5.4.

Figure 5.2.6.2 – Sketch of scour at bends (after Kirby et al. 2015)

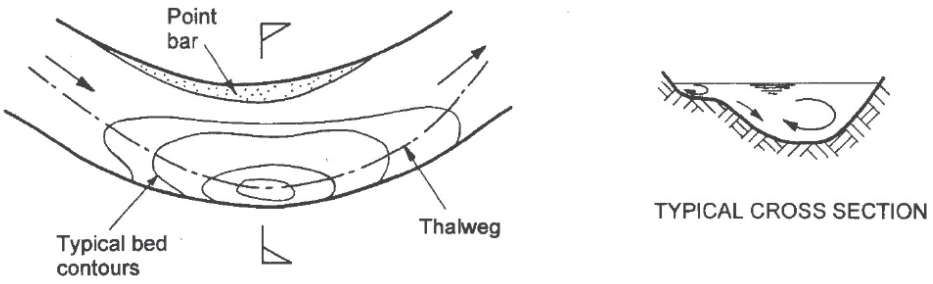

5.2.6.3 Confluence scour

Additional scour occurs at the confluence of two streams, where two streams of flow from converging channels meet at the centreline of the confluence, plunge to the channel bed, and then return to the water surface along the sides of the confluence. Channel confluence can increase scour at bridges due to the increase in sediment transport capacity caused by flow concentration at crossings (Melville and Coleman 2000). Despite the complexity of this phenomena, some efforts have been made to quantitatively assess confluence scour; these are briefly discussed in Section 5.4.

5.2.6.4 Sediment wave scour

Sediment waves occur at bridges during flows inducing sediment motion. The magnitude of these waves influence scour at bridges, as dune troughs temporarily lower local bed elevations. These waves can also significantly decrease conveyance at bridges. Melville and Coleman (2000) present methods to quantitatively predict scour due to sediment dunes.

The assessment of general scour is a specialist topic, as such it is recommended to seek advice from a river geomorphologist when evaluating it. Alternatively, some methods to evaluate general scour are discussed in Section 5.4. Further guidance and information are available in Melville and Coleman (2000) and Kirby et al. (2015).

5.2.6.5 Other types of scour

Other types of general scour relevant for bridges are:

- Pluvial scour - usually occurs behind bridge abutments as a result of localised pluvial runoff, while this scour is smaller in magnitude than local scour in rivers, it has the potential to initiate / aggravate scour at abutments, and
- Tidal scour – triggered by tidal flows and interaction of tidal and fluvial currents.

5.2.7 Contraction scour

Addition

Note that contraction scour does not account for localized scour at the foundations (local scour) or long-term changes in the stream bed elevation (aggradation or degradation).

Methods to estimate live-bed and clear-water contraction scour are presented in Sections 5.4.3 and 5.4.4 respectively.

While most literature refers to contraction scour and local scour at abutments independently, some methodologies that relate local scour at abutments to contraction scour have been recently developed (NCHRP 24-20, 2010), this is believed to be more physically representative of scour processes at abutments. This method is presented in Section 5.4.9.

5.2.8 Local scour

Addition

The flow field and maximum scour depths around bridge piers are dependent on three main variables:

1. effective pier width (including pier geometry and position in relation to flow)
2. flow depth, and
3. erodibility of the bed material.

Recent research has found that the flow fields around piers vary depending on the effective width of the pier in relation to the water depth (Melville and Coleman 2000; NCHRP, 2011a).

Figure 5.2.8(a) shows the main flow features of the flow field that usually occur around cylindrical piers for various water depths. The eroding forces exerted on the material supporting the pier are generated by flow contraction around the pier, by a pronounced down-flow at the pier's leading edge, and by turbulence structures of a wide range of turbulence scales. Variations of pier width and shape, and flow depth, alter the flow field, enhancing or weakening these flow features (NCHRP 2011a).

Note that the pier flow field may become more complicated if the pier has a complex shape or is in close proximity to an abutment and/or a channel bank.

In terms of values of y/a values (where a is the pier width and y is the flow depth) commonly encountered in the field, three categories of pier flow field, which produce significantly different pier scour morphologies are identified (Melville and Coleman 2000):

a) Narrow Piers ($y/a > 1.4$) for which scour typically is deepest at the pier face

b) Transitional Piers ($0.2 < y/a < 1.4$)

c) Wide Piers ($y/a < 0.2$) for which scour typically is deepest at the pier flank.

Narrow Piers - the main features of the flow field at narrow piers are an unsteady set of flow features that entrain and transport sediment from the pier foundation. They include: flow impact against the pier face, producing a down-flow and an up-flow with roller; flow converging, contracting, then diverging; the generation, transport and dissipation of large-scale turbulence structures (macro-turbulence) at the base of the pier-foundation junction (commonly named the horseshoe vortex); detaching shear layer at each pier flank; and, wake vortices convected through the pier's wake. The features evolve as scour develops (NCHRP 2011a).

In addition to the vertical component of flow at the pier's leading face, flow contracts as it passes around the sides of the pier and local values of flow velocity and bed shear stress increase. For many piers, the increases are such that scour begins at the sides of a pier. Once the scour region develops as a hole fully around the pier, the down-flow and the horseshoe vortices strengthen. Scour-hole formation draws flow into the hole.

Transition Piers - The main flow-field features described for narrow piers exist also in the flow field of piers within the transition range of y/a, but the features now begin to alter in response to reductions of y and or increases in a. The closer proximity of the water surface to the foundation boundary (for constant pier width), or the increased width of a pier (for constant flow depth), partially disrupt the formation of the features, and thereby reduce their capacity to erode foundation material. Though further research is needed to systematically describe and document the flow field changes, ample data show that reducing y/a results in shallower scour depths for this transition category of flow field (NCHRP 2011a).

Figure 5.2.8(a) depicts a sequence of flow field adjustments commensurate with three values of y/a, indicating how the scour capacity of flow field reduces as the flow depth, y, and consequently the value of y/a decrease. The down-flow at the pier face becomes less well developed because it has a shortened length over which to develop, whereas the up-flow associated with the (flow stagnation) bow wave remains essentially unchanged. The vorticity (circulation) of the large-scale turbulence structures (horseshoe vortex) which is aligned more-or-less horizontally in the pier flow field, weakens as the down-flow weakens, and the vertically aligned turbulence structures (wake vortices) also weaken due to the increased importance of bed friction in a shallower flow.

Wide Piers - For wide piers, the flow approaching the pier decelerates, turns, and flows laterally along the pier face before contracting and passing around the sides of the pier. The down-flow at the pier face is weakly developed, and only slightly erodes the foundation at the pier centreline. The circulation of the necklace vortices peaks at vertical sections situated around the flanks of the pier. Flow velocities near the pier are greatest where flow contracts around the pier's sides. Erosive turbulence structures now principally comprise wake vortices and the part of the horseshoe vortex system located in the scour region close to each flank of the pier. Deepest scour occurs at the pier flanks (NCHRP 2011a and c).

For a given flow depth, greater pier width increases flow blockage and therefore causes more of the approach flow to be swept laterally along the pier face than around the pier's flanks. Increased blockage modifies the lateral distribution of approach flow over a longer distance upstream of a pier.

Note that Figure 5.2.8(a) depicts the effect of flow depth changes for a constant pier width, this effect is different when the pier width changes for a constant flow depth.

Figure 5.2.8(a) – Variation of flow field with reducing approach flow depth (from Ettema et al. 2017)

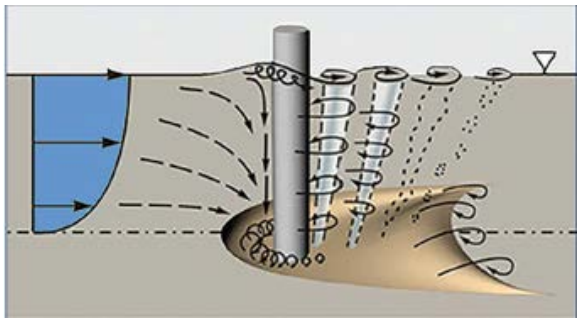

a) Narrow Pier (y/a > 1.4)

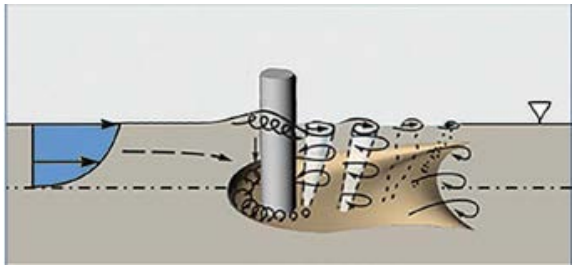

b) Transitional Pier (0.2 < y/a < 1.4)

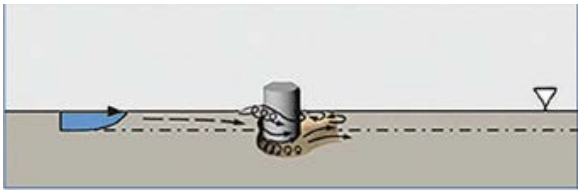

c) Wide Pier (y/a < 0.2)

Shallower flows (the flow field changes; turbulent structures weaken)

Methods to estimate clear-water and live-bed local scour at piers and abutments are presented in Section 5.4.

5.3 Bridge scour design and evaluation

5.3.1 General

Difference

Overtopping event plus an additional 300 mm in water surface is not mandatory in Queensland.

Events that should be used for scour estimation should be referred to as:

- Serviceability Limit States (SLS) for the bridge structure, and
- Ultimate Limit States (ULS) for structural strength and stability of the bridge structure.

Addition

A bridge is required to remain open (without damage) under various combinations of serviceability loads. Limit states can be related to the AEP of a flood event to quantify the damage caused during floods to bridges and structures.

ULS and SLS events specified by AS 5100.1 and the *Design Criteria for Bridge and Other Structures* (Transport and Main Roads, March 2017) are listed in Table 5.3.1 where the department's design criteria takes precedence over AS 5100.1.

Table 5.3.1 – Serviceability and Ultimate Limit States (ULS)

Type of Road	AS 5100.1		Transport and Main Roads 2017	
	SLS	ULS	SLS	ULS
State controlled roads	1% AEP	0.05% AEP	1% AEP	0.05% AEP or overtopping event if less than 0.05% AEP, whichever is critical in terms of flood forces*

*If the overtopping event is greater than SLS or 1% AEP but smaller than the 0.05% AEP event, a risk assessment to determine if the scour protection should be designed to withstand the overtopping event (instead of the SLS) must be conducted.

The SLS flood event shall not cause damage to the bridge, abutment, road embankment (including the load effect of piers and abutments). The structural integrity of bridges shall not be compromised by any flood up to and including the ULS flood event, including the effect of ULS scour level, all loads specified in AS 5100.1 and AS 5100.2.

5.3.2 New bridges

Addition

Two-dimensional (2D) models should be used on all but the simplest bridge crossings as a matter of course (Arneson et al. 2012). While two-dimensional models cannot replicate pressurized flow conditions, they better replicate flow contraction and expansion patterns occurring at bridges. For overtopping bridges pressure scour shall be accounted for in addition to local / contraction scour estimates. It should be noted that while 1D models such as HEC-RAS might account for pressurized flow in bridges, they might not necessarily calculate pressurized flow (vertical contraction) scour. In addition, Computational Fluid Dynamics (CFD) models might also be used to conduct forensic investigations of historic failures (M. Jacobs, personal communication, December 2018) or validate results at complex bridge structures.

Scour at relevant floods shall be considered within bridge design. Design of bridge piers shall not rely on pier scour protection, they shall be designed considering estimated maximum scour depths at piers to ensure the structural integrity of the bridge under the action of scour. Scour protection should not be installed around new bridge piers (TMR 2018a).

Bridge abutments shall be designed by taking into consideration possible scour determined by scour analysis. Abutments and road approaches shall be adequately protected to prevent scour for floods up

to the SLS event. However, any scour protection designed for SLS conditions, shall not be relied upon at the ULS event (as per Clause 11.1, AS 5100.1:2017).

Excluding spread footings founded on solid rock, minimum scour depth for ULS design shall be 2 m measured from the bottom of the headstock. The bridge shall be designed for worst ultimate flood forces up to 0.05% AEP event without relying on abutment protection. If the bridge is closed to traffic under ULS conditions, the accompanying traffic loads on the bridge can be excluded (as per Clause 23.3, AS 5100.2:2017).

In addition to the scour analysis conducted by the hydraulic engineer, a geotechnical engineer shall be consulted when determining the maximum design scour depths at the bottom of the abutment headstock to use for bridge design. The work in both disciplines shall be conducted under the direction of an experienced RPEQ engineer in each field.

The limiting depth of abutment scour when the geotechnical stability of the bridge embankment is reached, shall also be considered when calculating abutment scour depths (see Figure 5.4.9(b). The geotechnical engineer designing the abutments should be consulted regarding this limit.

Scour protection at piers and abutments shall be designed based on the maximum average cross sectional velocity for floods up to the ULS event, and shall consider situations such as:

- overtopping bridge and bridge embankment
- effects of local catchments and along road drainage, and
- scour analysis based on actual particle size of bed material and bed shear stress (in sand, scours to more than 5 m are common, TMR 2018a).

In some situations, maximum localised velocities at abutments and piers might provide more accurate information on velocities required for design. Engineering judgement shall always be exercised to endorse large velocities potentially created by two-dimensional model instabilities. On site observations and evidence of previous scour often help to validate calculated velocities.

Potential scour at approach embankments should also be considered when designing overtopping bridges.

It should be noted that while most available methods relate scour to flow velocity, the critical force causing scour is the bed shear stress, defined as the shear force per unit area exerted on the channel bed by flowing water. This force is maximum at the channel bed and banks where the velocity is zero. As for velocities, practitioners must be aware of the differences between average and point shear stresses.

1D models (e.g. HEC-RAS 1D, etc.) cannot calculate localised bed shear stresses at bridges and as such should not be used in the design of scour protection. 2D models provide better identification of the distribution of velocities and bed shear stresses around bridges but can only account for horizontal changes in flow direction. Consequently, bed shear stresses around piers and abutments (where helical vortexes and other flow structures that can cause scour, occur) can only be accurately calculated using CFD models, which allow for horizontal and vertical changes in flow direction.

While CFD modelling of bridges is not widely practiced in Australia, some efforts have been recently conducted by Transport and Main Roads to validate bridge loss factors (commonly used in 2D modelling to represent losses due to bridges) and for forensic analysis of historic failures. Results from these studies indicate that the technique is reliable and can add to the development of robust engineering designs of complex bridge structures.

Due to the large number of CFD modelling packages available, it is not desirable or practical to prescribe CFD modelling parameters within this document. However, the following general guidelines (M. Jacobs, personal communication, December 2018) may be used when bed shear stresses are required for a bridge design under SLS conditions, which assumes fully developed scour holes at the piers, but intact scour protection at the abutments:

- The primary purpose of the CFD model should be to calculate bed shear stresses and other flow parameters under steady-state conditions occurring under peak flows. Boundary conditions should reflect flows and water levels occurring under peak flow conditions only, these boundary conditions should be estimated from the outcomes of separate 1D or 2D models. CFD models should not be used to estimate flood levels.
- The CFD model should cover the area of interest around the bridge. The model boundaries should be set at sufficient distance to not significantly affect flow conditions at the bridge. As a guide, the boundaries should be a minimum distance of 2 bridge spans upstream and 4 bridge spans downstream, depending on the geometry of the bridge and channel.
- CFD models are computationally intense. The ratio run-time to simulated-time can be about 50 or 100 to 1. Further, flow systems can take some time to stabilize. It is not uncommon to observe unrealistic see shock-waves travel through a model at the start of the simulation. For practical purposes, then, it is suggested that models be run for short periods of simulated time, to allow the flow to approximate steady state conditions, and report results at the end of the simulation.
- While it is possible to model mobile beds, a fixed bed might be initially assumed for the purposes of mapping bed shear stresses at the point of scour inception. Fully developed scour holes at the bridge piers might then be added to the model mesh. The dimensions of these scour holes may be estimated by the techniques described elsewhere in this supplement or calculated modelling a mobile bed.
- The estimated bed shear stresses should be compared with the allowable shear stresses of the in-situ or engineered material at the bed to assess whether further modification of the bed is required.
- CFD models should include decks, railing and debris rafts (if required), to accurately model the effects of pressurised flow on bed shear stresses.
- CFD models should be calibrated and/or at least validated against other methodologies.
- Sensitivity testing is recommended, to assess how the cell sizes affect outcomes, particularly estimated bed shear stresses. Sensitivity of the used turbulence model might also be required.

5.3.3 Existing bridges

Addition

Critical scour levels at piers and abutments in terms of structural integrity shall be considered, and a multidisciplinary risk assessment (including structural, geotechnical and hydraulic engineers) conducted to decide at which stage countermeasures are required. Countermeasures for approach embankments prone to scour must also be considered. Periodical monitoring shall be conducted at bridges where scour is present. Section 5.6 describes several techniques available to monitor scour.

On site observations and evidence of previous scour are always useful when designing scour mitigation measures for existing bridges.

5.3.4 Design procedures for abutment protection

Accepted

5.3.5 Foundation to resist scour

Accepted

5.3.6 Evaluation of foundation design for ULS scour

Accepted

5.3.7 Scour related to construction

Addition

Whiteridge (2017a, b) presents a comprehensive guideline on measures to prevent erosion during road construction.

5.4 Methods of estimating scour

5.4.1 General

Addition

Melville and Coleman (2000) and Kirby et al. (2015) are additional reference documents that present methods to calculate scour at bridges.

5.4.2 Design approach

Addition

Before embarking on the calculation of scour depths it is recommended to conduct an initial assessment of the scour risk that the subject bridge poses.

This initial assessment should identify evidence of previous scour and other parameters that might influence scour at the subject location (that is, bridge near a bend or confluence, steep stream slope or likely high velocities), likelihood of scour at founding material and advice on the soundness of the proposed type / depth of bridge foundations. It is advisable to involve a river geomorphologist in this initial assessment of the likelihood of aggradation / degradation, lateral movement, and other general / natural scour processes. For existing bridges, this assessment shall also include if satisfactory foundation and scour protection is provided.

Bridges may be classified as low risk in terms of scour if they are located outside the floodplain or are founded on erosion resistant material; as such the soil profile information (including soil types and Standard Penetration Test Results (SPTs) under the bridge is necessary to accurately conduct this initial assessment. At bridges where the founding material is unknown, a detailed scour assessment that involves calculating the potential total scour depth shall be conducted. The below diagram depicts the recommended scour assessment methodology.

Total scour depths at piers and abutments shall be plotted in a General Arrangement (GA) drawing next to the geotechnical profiles estimated from borehole logs by a geotechnical engineer based on type of soil and Standard Penetration Test values (SPTs). This drawing shall be included as a deliverable within the set of bridge drawings issued for reviews, approval and construction (refer to drawings provided in worked examples).

Figure 5.4.2 – Recommended scour assessment methodology

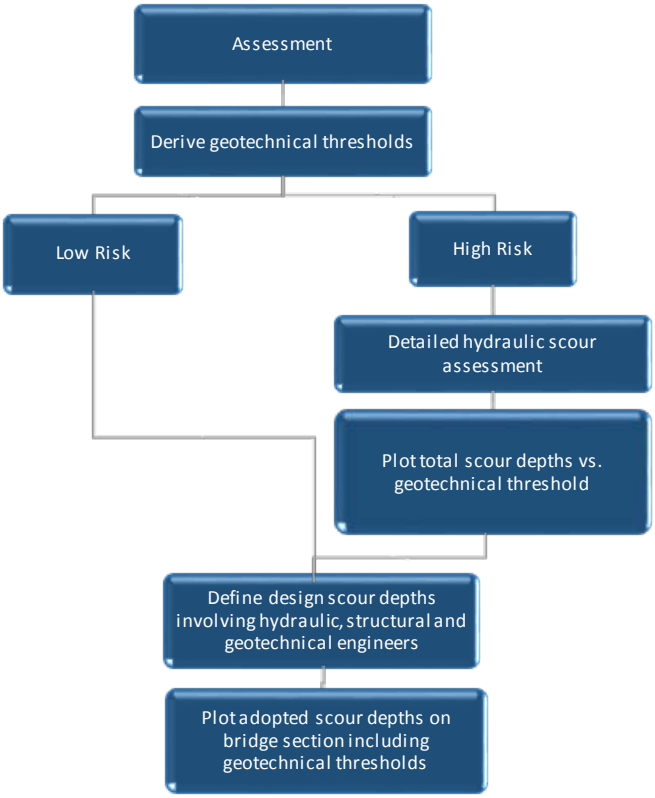

Natural scour refers to the changes in bed levels that occur due to natural (non-anthropogenic) factors without any additional effects caused by the presence of structures. Natural scour is difficult to predict due to the complex interaction between riverine sediment transport processes and potential catchment / stream changes.

5.4.2.1 Degradation

Degradation is defined as the lowering of bed level along the main channel of a river and usually occurs over a period of years. No simple procedures for estimating changes in bed level exist because degradation is caused by large scale imbalances in sediment load and supply and is dependent on the geotechnical properties of the stream. Kirby et al. (2015) recommend four methods to estimate degradation in channels:

1. Collection of historical and field data – qualitative assessments of aggradation conducted by an experienced river geomorphologist and based on past and current trends can effectively identify potential stream stability problems.
2. Use of regime equations – these equations calculate dimensions of a regime channel corresponding to bankfull flow, if the predicted characteristics of the channel are significantly different from existing channel geometry, the channel may not be stable and may tend to evolve towards the regime properties (unless prevented by geological features and/or training works).
3. Use of threshold methods – these equations calculate channel threshold conditions in terms of velocity, shear stress or stream power.

4. Numerical models – 1D or 2D morphological models may be used to predict long term changes, however it must be noted that these models require extensive input data and assumptions on sediment transport processes. Advice from a suitably qualified fluvial geomorphologist is recommended when using sediment transport models.

Due to uncertainty in calculating general / natural scour, input from a river geomorphologist is strongly recommended to estimate it either qualitatively or quantitatively.

Some of the most used regime equations are herein reproduced. Note that these equations predict the mean flow depth at regime (measured from the water surface to the channel bed).

Where the variation of water surface level with flow rate is known, Neill (1973) indicates that degradation levels at a bridge site in an uncontracted alluvial river can be calculated with the regime formula of Lacey (1930).

$$Y_{ms} = 0.47\left(\frac{Q}{f}\right)^{1/3} \qquad \text{Equation 5.4.2.1(a)}$$

Where:

Q is the bankfull discharge (m^3/s)

f is the Lacey silt factor, denoted as $f = 1.76d_m^{0.5}$

d_m is the mean diameter of the bed material in millimetres, and

Y_{ms} is the mean flow depth at regime in metres (measured from the water surface to the channel bed)

This method was derived for uncontracted sandy alluvial channels; as such it might give excessive scour depths for more resistant materials. For sandy materials f should be taken as 1 (Neill, 1973).

Blench (1969) provides another regime formula to determine scour depths for sand streams:

$$Y_{ms} = 1.2\left[\frac{q^{2/3}}{d_{50}{}^{1/6}}\right] \qquad 0.06mm < d_{50} < 2mm \qquad \text{Equation 5.4.2.1(b)}$$

$$Y_{ms} = 1.23\left[\frac{q^{2/3}}{d_{50}{}^{1/12}}\right] \qquad S_g = 2.65 \; and \; d_{50} > 2mm \qquad \text{Equation 5.4.2.1(c)}$$

Where:

q is the bankfull discharge of the main channel per unit width ($m^3/s/m$)

d_{50} is the sediment size for which 50% of the sediment is finer in metres

S_g is the specific gravity of the rock (usually taken as 2.65), and

Y_{ms} is the mean flow depth including scour (measured from the water surface to the channel bed) in metres

This method was derived for real in-regime hydraulically smooth canals of steady discharge, very small steady sediment transport rate and suspended load, as such Equation 5.4.2.1(b) applies to most sand bed irrigation canal systems while Equation 5.4.2.1(c) was derived for large gravel rivers.

Other methods to qualitatively assess general scour can be found in Kirby et al. (2015) and Melville and Coleman (2000).

5.4.2.2 Bend scour

Flow around a river bend creates a non-uniform flow distribution with outer bend velocities being higher than those in the straight sections of the channel. A spiral flow secondary current transporting bed sediment towards the inside bend also occurs. Consequently, the flow depth around the outer bend is usually greater than the average depth in a straight channel and the depth around the inside of the bend is smaller than average depths in a straight channel (Kirby et al. 2015).

The equations provided by Maynord (1996) and Thorne (1988) recommended by Melville and Coleman (2000) are listed below. Note that these equations were obtained for in bank flows (refer to Figure 5.4.2(a):

$$\frac{Y_{bs}}{Y_u} = 1.8 - 0.051\left({}^{r_c}/_{W}\right) + 0.0084\left({}^{W}/_{Y_u}\right) \; for \; 1.5 < {}^{r_c}/_{W} < 10 \; and \; 20 < {}^{W}/_{Y_u} < 125 \quad \text{Equation 5.4.2.2(a)}$$

$$\frac{Y_{bs}}{Y_u} = 2.07 - 0.19\ln\left[\left({}^{r_c}/_{W}\right) - 2\right] for \; {}^{r_c}/_{W} > 2 \quad \text{Equation 5.4.2.2(b)}$$

Where:

Y_{bs} is the depth at bend in metres

Y_u is the average flow depth in the channel upstream of the bend in metres

W is the flow width in metres and

r_c is the centreline radius of the bed in metres

Maynord (1996) recommends the adoption of a safety factor due to the non-conservativeness of his method. He recommends factors of 1, 1.08 and 1.19 for 25%, 10% and 2% uncertainty. He also recommends adopting $r_c/W=1.5$ for values of $r_c/W < 1.5$ and $W/Y_u = 20$ for values of $W/Y_u < 20$.

Figure 5.4.2(a) – Variation of flow depth in a bend (after Melville and Coleman 2000)

5.4.2.3 Confluence scour

When two rivers meet at a confluence, rapid changes in fluid velocity and turbulence intensity can cause bed geometry changes. Usually, a deep scour hole and a depositional point bar are present at the confluence. Similar effects may also occur where two channels in a braided river combine.

Ashmore and Parker (1983) and Klaasen and Vermeer (1988) present the below equation to calculate confluence scour.

$$\frac{Y_{cs}}{\bar{y}} = C_0 + C_1\theta \quad \text{Equation 5.4.2.3}$$

Where:

Yc_s is the depth just downstream of the confluence in metres

$\bar{y}$ is the average flow depth in the main anabranch in metres

C_0 is 1.29 and C_1 is 0.037 for rivers with fine sands, 2.24 and 0.031 for rivers with coarse sands and gravels and 1.01 and 0.03 in cohesive material and θ is the angle between anabranches in degrees

Figure 5.4.2.3 – Flow depth at a confluence (after Melville and Coleman 2000)

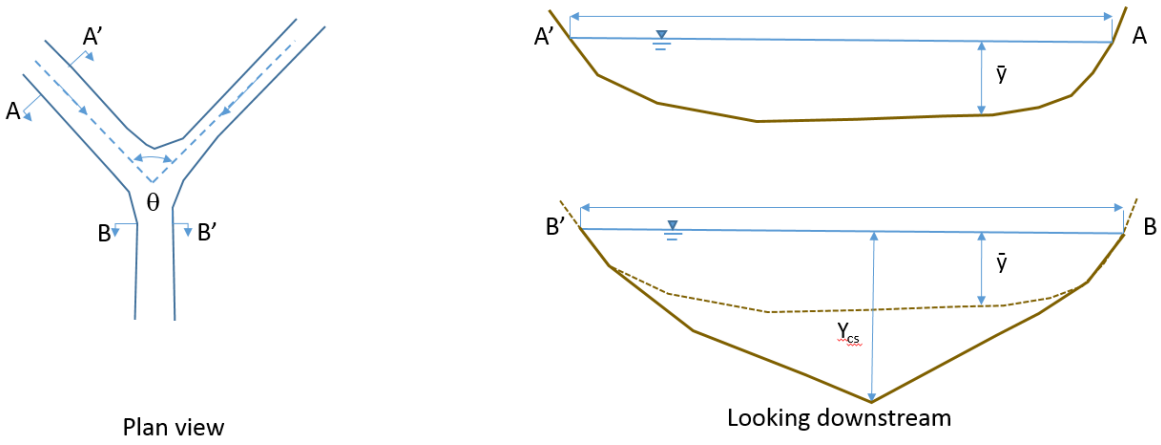

Other general / natural scour processes such as lateral erosion / channel migration and sediment-wave erosion are documented in Melville and Coleman (2000) and Kirby et al. (2015).

5.4.3 Live-bed contraction scour

Addition

There are four conditions (cases) of contraction scour at bridge sites depending on the type of contraction, and whether there is overbank flow or relief bridges (refer to Section 5.2.7). Regardless of the case, contraction scour can be evaluated using two basic equations: the live-bed scour equation (Equation 33, Austroads, 2018), and the clear-water scour equation (Equation 35, Austroads, 2018).

For any case or condition, it is only necessary to determine if the flow in the main channel or overbank area upstream of the bridge, or approaching a relief bridge, is transporting bed material (live-bed) or is not (clear-water), and then apply the appropriate equation with the variables defined according to the location of contraction scour (channel or overbank).

To determine if the flow upstream of the bridge is transporting bed material, the critical velocity for beginning of motion V_c of the d_{50} size of the bed material being considered for movement and should be calculated and compared to the mean velocity V of the flow in the main channel or overbank area upstream of the bridge opening.

If the critical velocity of the bed material is larger than the mean velocity ($V_c > V$), then clear-water contraction scour will exist. If the critical velocity is less than the mean velocity ($V_c < V$), then live-bed contraction scour will exist. Equation 5.4.3(a) below can be used to calculate the critical velocity (Arneson et al. 2012):

$$V_c = K_u y^{1/6} {D_{50}}^{1/3} \qquad \text{Equation 5.4.3(a)}$$

Where:

V_c = critical velocity above which bed material of size d and smaller will be transported, (m/s)

y = average depth of flow upstream of bridge, (m)

d_{50} = Particle size in a mixture of which 50 percent are smaller, (m)

K_u = 6.19 (SI units)

5.4.4 Clear-water contraction scour

Accepted

5.4.5 Contraction scour with backwater

Accepted

5.4.6 Contraction scour in cohesive materials

Difference

The bridge entrance is also referred to as the upstream face of the bridge.

Initial shear stress can be calculated using Equation 37 in Austroads, 2018. If the shear stress does not exceed the critical value for that material (from test data or Figure 5.23, Austroads 2018), then no contraction scour will occur during that flow period. If the critical shear is exceeded, then ultimate scour for that flow condition can be computed using Equation 36 in Austroads, 2018 (after Briaud et al. 2011).

5.4.7 Contraction scour in erodible rock

Addition

A geotechnical engineer's interpretation of the soil characteristics (for example, soil types and Standard Penetration Test Results (SPTs) is necessary to accurately deem material as erosion resistant.

5.4.8 Mean velocity method

Addition

At locations where significant floodplain flows occur, results from two-dimensional models can be used to identify the width of flows likely to carry sediment. Plotting 2D velocities and unit discharges at the vicinity of the bridge provides an idea of the conveyance of the main channel and floodplain fringe and helps to determine flows that are likely and unlikely (for example, shallow and slow flows) to transport sediment and contribute to scour.

5.4.9 Scour at abutments

Addition

NCHRP (2010b) developed abutment scour equations considering a range of abutment types, locations, flow and sediment transport conditions. These equations use contraction scour as the starting calculation for abutment scour and apply a factor to account for large-scale turbulence that develops in the vicinity of the abutment.

Due to the non-uniform flow distribution created by the abutment in the contracted section, the flow is more concentrated in its vicinity and the contraction scour component is greater than for average conditions in the constricted opening. The three scour conditions illustrated in Figure 5.4.9(a) are:

a) scour occurring when the abutment is in or close to the main channel

b) scour occurring when the abutment is set back from the main channel, and

c) scour occurring when the embankment breaches and the abutment foundation acts as a pier.

The NCHRP study also concluded that there is a limiting depth of abutment scour when the geotechnical stability of the embankment or channel bank is reached (see Figure 5.4.9(b). The geotechnical engineer designing the abutments should be consulted regarding this limit.

The abutment scour computed using the NCHRP approach is total scour at the abutment; and should not be added to contraction scour because it already includes contraction scour.

Figure 5.4.9(a) – Abutment scour conditions (after NCHRP, 2010b)

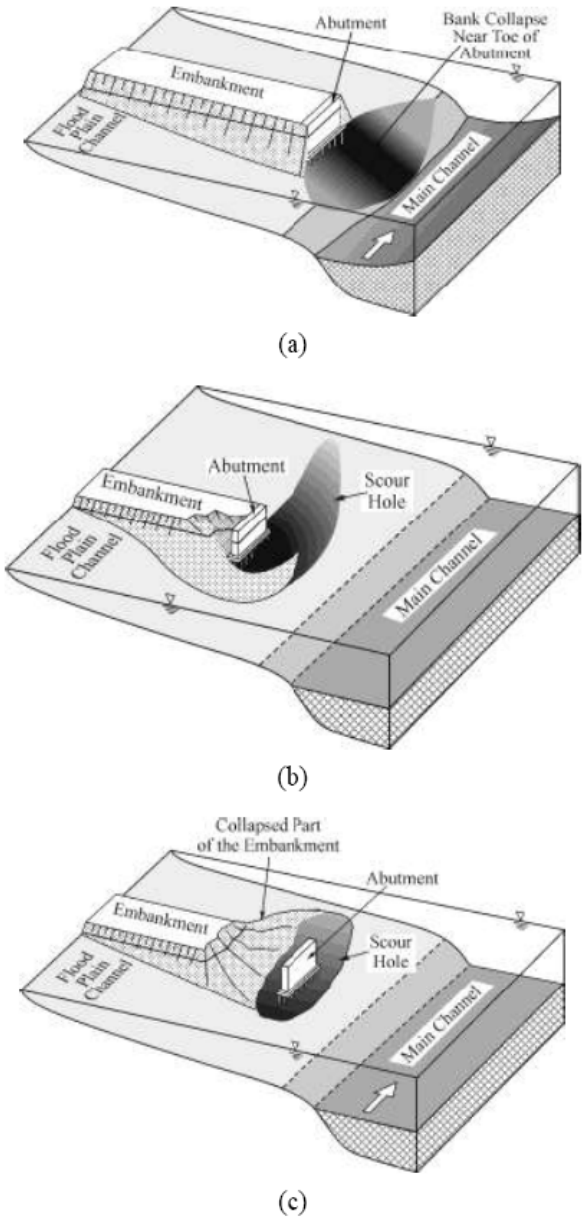

Figure 5.4.9(b) – Conceptual geotechnical failure resulting from abutment scour (after NCHRP, 2010b)

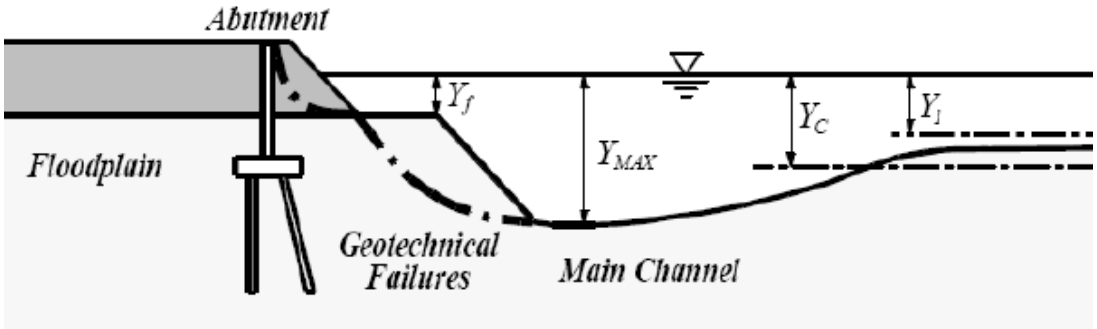

The advantages of using the NCHRP abutment scour equations include:

1. not using the effective embankment length, L', which is difficult to determine in many situations
2. the equations are more physically representative of the abutment scour process, and
3. the equations predict total scour at the abutment rather than the abutment scour component that is then added to contraction scour.

The abutment contraction scour equations for live-bed and/or clear-water conditions are:

$$Y_{max} = \alpha_A \cdot Y_C \quad (live-bed) \quad or \quad Y_{max} = \alpha_B \cdot Y_C \quad (clear-water) \qquad \text{Equation 5.4.9(a)}$$

$$Y_s = Y_{max} - Y_0 \qquad \text{Equation 5.4.9(b)}$$

Where:

Y_{max} = Maximum flow depth resulting from abutment scour, (m)

Y_c = Flow depths including live-bed or clear-water contraction scour, (m)

α_A = Amplification factor for live-bed conditions

α_B = Amplification factor for clear-water conditions

Y_s = Abutment scour depth, (m)

Y_0 = Flow depth prior to scour, (m)

Based on the NCHRP (2010b) study, if the projected length of the embankment, L, is 75 percent or greater than the width of the floodplain (B_f), scour condition (a) in Figure 5.4.9(a) occurs and the contraction scour calculation is performed using a live-bed scour calculation.

The contraction scour equation is a simplified version of the live-bed contraction scour equation (Equation 33, in Austroads 2018). The equation combines the discharge and width ratios due to the similarity of the exponents because other uncertainties are more significant. This simplifies the live-bed contraction scour equation to the ratio of the unit discharge upstream and at the constricted section of the bridge (q_1 and q_{2C}), where q_{2C} is the total discharge in the bridge opening divided by the width of the bridge opening and q_1 is the upstream unit discharge estimated either by dividing discharge by width or by the product of velocity and depth upstream of the bridge.

The contraction scour equation becomes:

$$Y_c = Y_1 \left(\frac{q_{2c}}{q_1}\right)^{6/7} \qquad \text{Equation 5.4.9(c)}$$

Y_c = Flow depth including live-bed contraction scour, (m)

Y_1 = Upstream flow depth, (m)

q_1 = Upstream unit discharge, (m²/s)

q_{2c} = Unit discharge in the constricted opening accounting for non-uniform flow distribution, (m²/s)

The value of Y_c is then used in Equation 5.4.9(a) to compute the total flow depth at the abutment. The value of α_A is selected from Figure 5.4.9(c) for spill through and wingwall abutments where the solid curves should be used for design, as dashed curves represent theoretical conditions that have yet to be proven experimentally.

These experimental curves show that for low values of q_2/q_1, contraction scour is small but the amplification factor is large because flow separation and turbulence dominate the abutment scour process. For large values of q_2/q_1, contraction scour dominates the abutment scour process and the amplification factor is small.

If the projected length of the embankment, L, is less than 75 percent of the width of the floodplain (B_f), scour condition (b) occurs (refer to Figure 5.4.9(a)) and the contraction scour calculation is performed using the clear-water scour equation (Equation 35, in Austroads, 2017). The standard clear-water contraction scour equation also uses the unit discharge (q), which can be estimated either by dividing the discharge by width or by the product of velocity and depth. Two clear-water contraction scour equations may be applied. The first equation is the standard equation based on grain size:

$$Y_c = \left(\frac{q_{2f}}{K_u D_{50}^{1/3}}\right)^{6/7} \qquad \text{Equation 5.4.9(d)}$$

Where:

Y_c = Flow depth including clear-water contraction scour, (m)

q_{2f} = Unit discharge in the constricted opening accounting for non-uniform flow distribution, (m^2/s)

K_u = 6.19 (SI)

d_{50} = Particle size with 50% finer, (m)

Note that a lower limit of particle size of 0.2 mm is reasonable because cohesive properties limit the critical velocity and shear stress for cohesive soils.

When using Figure 5.4.9(a) above and Figure 5.4.9(c), the value of q_{2f} should be estimated including local concentration of flow at the bridge abutment while the value of q_f is the floodplain flow upstream of the bridge. The value of Y_c is then used in Equation 5.4.9(a) to compute the total flow depth at the abutment. The value of α_B is selected from Figure 5.4.9(c) for spill through and wingwall abutments. Once again, the solid curves should be used for design, as the dashed curves represent theoretical conditions that have yet to be proven experimentally.

If the critical shear stress is known for a floodplain soil, then an alternative clear-water scour equation can be used. For further details of this equation refer to Section 8.6.3 of Arneson et al. (2012).

For scour estimates determined for either condition (live-bed and clear-water) the geotechnical stability of the channel bank or embankment should be considered. If the channel bank or embankment is likely to fail, then the limiting scour depth is the geotechnically stable depth and erosion will progress laterally. This may cause the embankment to breach and another scour estimate can be performed treating the abutment foundation as a pier.

It should be noted that there are many uncertainties in determining the variables for these abutment scour equations. Determining the grain size or critical shear stress of the floodplain soils is one source of uncertainty. Determining the value of unit discharge near the abutment is another source of uncertainty.

The length of embankment blocking ‘live’ flow can be determined by plotting the unit discharge / conveyance at the upstream vicinity of the bridge where low velocity and/or shallow flows at the ineffective flow areas upstream of bridge are unlikely to transport sediment and significantly

contribute to contraction scour, as such the length of embankment blocking this flow should not be used for abutment scour.

Two-dimensional models provide much better estimates of conveyance throughout the bridge opening than one-dimensional models, as they can be calculated at any point in the two-dimensional flow field by multiplying velocity and depth. As such, the recommended procedure for selecting the velocity and unit discharge for abutment scour calculation is to use two-dimensional modelling.

Figure 5.4.9(c) – Scour amplification factor for abutments under live-bed and clear water-conditions (NCHRP, 2010b)

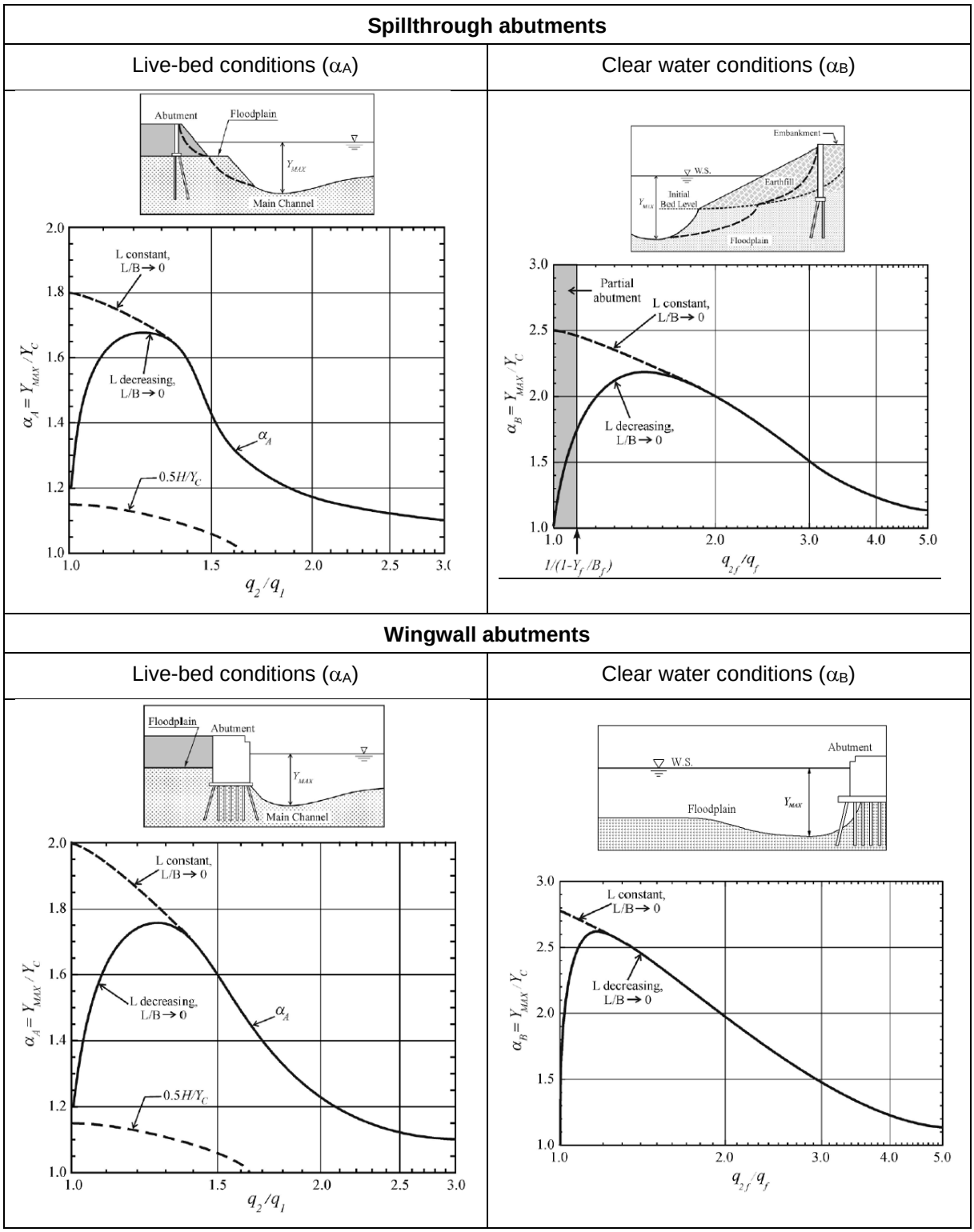

5.4.10 Local scour at piers

Difference

For scour computation in real world waterway bridges, viscosity and surface tension can be ignored.

5.4.10.1 Alternative methodologies

Non-dimensional local scour methodology (Melville and Coleman 2000)

This method was developed to predict local scour in both piers and abutments, it takes into account the various parameters influencing local scour (for example, shape and orientation of the structure, bed sediment, approach flow, and so on). The equation resulting from this method is shown below:

$$Y_s = K_{yB} K_I K_d K_s K_\theta K_G K_t \qquad \text{Equation 5.4.10.1}$$

Where Y_s denotes local scour depth and the K's are empirical factors accounting for the parameters influencing local scour, depth – size ratio for piers (K_{yB}) or abutments (K_{yL}), flow intensity (K_I), sediment size (K_d), pier or abutment shape (K_s), pier or abutment alignment (K_θ), channel geometry (K_G) and time (K_t). The parameters in the above equation and the way to calculate them are documented in (Melville and Coleman 2000). The rules of thumb recommended in Austroads (2018) for maximum local scour depth are derived from this methodology ($Y_s < 2.4b$ for $Fr < 0.8$ and $Y_s < 3.0b$ for $Fr > 0.8$).

Note that this methodology allows to take into account non-uniformity of piers based on the study of local scour at non-uniform circular piers (with diameter a) founded on larger circular caissons (with diameter a*) conducted by Raudkivi and Melville (1996).

Florida Department of Transport Pier Scour Methodology (FDOT, 2011)

Equation 42 and Equation 43 which were developed and modified over several decades have been used for bridge scour evaluations and bridge design for countless bridges worldwide. However, Arneson et al. (2012) note that these equations can be improved by including bed material size and a more detailed consideration of the bridge pier flow field (see Section 5.2.8).

Two NCHRP studies (NCHRP 2011a and 2011c) evaluated several pier scour equations and found that the Sheppard and Miller (2006) equation generally performed better than Equation 43 for both laboratory and field data. The results of the above NCHRP studies were evaluated and expanded into a pier scour analysis methodology by the Florida Department of Transport (FDOT) and published in their *Bridge Scour Manual* (FDOT, 2011). Supporting spreadsheets (available from the FDOT website) were also developed for a wide range of pier scour applications.

FDOT methodology includes flow velocity, depth and angle of attack, pier geometry and shape, but also includes particle size. Sheppard et al. (2011) states that the FDOT formula yields the most accurate prediction of scour at single piers to date, as it is based on a more complete dimensional analysis than Equation 43. As such, it should be considered as an alternative, particularly for wide piers in shallow flows with fine bed material ($y/a < 0.2$ as described in Section 5.2.8). The FDOT methodology is presented in detail in Section 7.3 of Arneson et al. (2012).

5.4.10.2 Scour at wide piers

Flume studies on scour depths at wide piers in shallow flows and field observations of scour depths at bascule piers in shallow flows indicate that existing pier scour equations, including Equation 43, overestimate scour depths (Arneson et al. 2012).

TRB 1994 suggests the following equations for a Kw factor to be used to correct Equations 42 or 43 for wide piers in shallow flow where the ratio of depth of flow to pier width (y/a) is less than 0.8 (y/a < 0.8); the ratio of pier width (a) to the median diameter of the bed material (d_{50}) is greater than 50 ($a/d_{50} > 50$); and the flow is subcritical (Froude Number < 1).

$$K_w = 2.58\left(\frac{y}{a}\right)^{0.34} Fr_1{}^{0.65} \qquad for\ \frac{V}{Vc} < 1 \qquad \text{Equation 5.4.10.2(a)}$$

$$K_w = 1.0\left(\frac{y}{a}\right)^{0.13} Fr_1{}^{0.25} \qquad for\ \frac{V}{Vc} \geq 1 \qquad \text{Equation 5.4.10.2(b)}$$

where K_w is the correction factor to Equations 42 or 43 for wide piers in shallow flow.

Engineering judgment should be used in applying K_w because it is based on limited data from flume experiments. Engineering judgment should take into consideration the volume of traffic, the importance of the highway, cost of a failure (potential loss of lives and dollars) and the change in cost that would occur if the K_w factor is used.

FDOT methodology is recommended for wide piers in shallow flows with fine bed material (y/a < 0.2 as described in Section 5.2.8) while Melville and Coleman (2000) methodology is recommended for non-uniform circular piers founded on larger circular caissons.

5.4.10.3 Scour for complex pier foundations

Most pier scour research has focused on solid piers with limited attention to the determining scour depths for pile groups, pile groups and pile caps, or pile groups, pile caps and solid piers exposed to the flow. These three types of exposure to the flow may be by design or by scour (long-term degradation, general (contraction) scour, and local scour, in addition to stream migration.

Some limited research has provided methods and equations to determine scour depths for complex pier foundations as an extension of the pier scour equations for routine cases (Equations 42 and 43). Results of this research are presented in the Section 7.5 of Arneson et al. (2012). However, it must be noted that engineering judgment is essential when applying the equations presented in this section as well as in deciding when a more rigorous level of evaluation is warranted.

Effectively, total scour depth for complex pier configurations is determined by separating the scour producing components, determining the scour depth for each component and adding the results. This method is called ‘Superposition of the Scour Components’ (refer to Figure 5.4.10.3). Section 7.5 of Arneson et al. (2012) for further details on this methodology.

Steps recommended to determine scour depths of any combination of flow exposed substructural elements (Jones and Sheppard, 2000) are herein reproduced:

1. Analyse the complex pile configuration to determine the components of the pier that are exposed to the flow or will be exposed to the flow which will cause scour.
2. Determine the scour depths for each component exposed to the flow using the equations and methods presented in the following sections.
3. Add the components to determine the total scour depths.
4. Plot the scour depths and analyse the results using an interdisciplinary team to determine their reliability and adequacy for the bridge, flow and site conditions, safety and costs.
5. Conduct a physical model study, if engineering judgment determines it will reduce uncertainty, increase the safety of the design and/or reduce cost.

Figure 5.4.10.3(a) – Scour components at a complex pier configuration (Arneson* et al*. 2012)

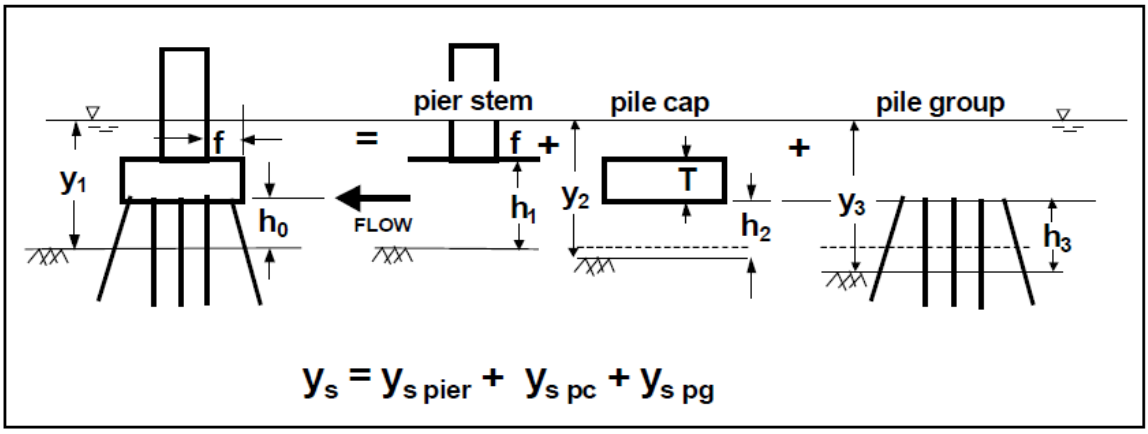

Sheppard et al. (2011) states that the superposition method neglects the influence of sediment coarseness and incipient motion, and its wide-pier correction leads to discontinuity among predicted results. An additional disadvantage of the superposition method is its separation of the pier components (NCHRP, 2011a), which in some cases can lead to underestimation.

The FDOT methodology (FDOT, 2011) can also be used to calculate scour at complex piers, it has a similar approach of decomposing the pier into three layers but considers the effective width of the pier instead of considering the cumulative effect of each component. Moreno et al. (2016a) propose equations for complex piers aligned with the flow while a recent experimental study from Yang et al. (2018) proposes equations (based on the FDOT methodology) that consider the effect of skewness on clear-water scour for complex pier configurations. Results from this latest study indicate that pile cap elevations and pier skewness significantly affect the scour depth with even a slight skewness significantly increasing scour depths at complex piers.

Physical model studies are still recommended for complex piers with unusual features such as staggered or unevenly spaced piles or for major bridges where conservative scour estimates are not economically acceptable.

Pier scour in cohesive material

Addition

Briaud et al. (2011) developed Equation 5.4.10.3 to calculate pier scour in cohesive materials, which incorporates the critical velocity for initiation of erosion:

$$Y_s = 2.2K_1K_2a^{0.65}\left(\frac{2.6V_1-V_c}{\sqrt{g}}\right)^{0.7} \qquad \text{Equation 5.4.10.3}$$

where Y_s, K_1, K_2, a, and V_1 are defined as in Equation 43 of Austroads (2018) and V_c is the critical velocity for the onset of erosion of the cohesive material in m/s. This velocity can be determined through material testing (see Briaud et al. 2011) or using an erosion rate of 0.1 mm/hr from Figure 5.4.10.3(b) for various types of materials.

Figure 5.4.10.3(b) – Erosion rate vs. velocity for a wide range of materials (Briaud et al. 2011)

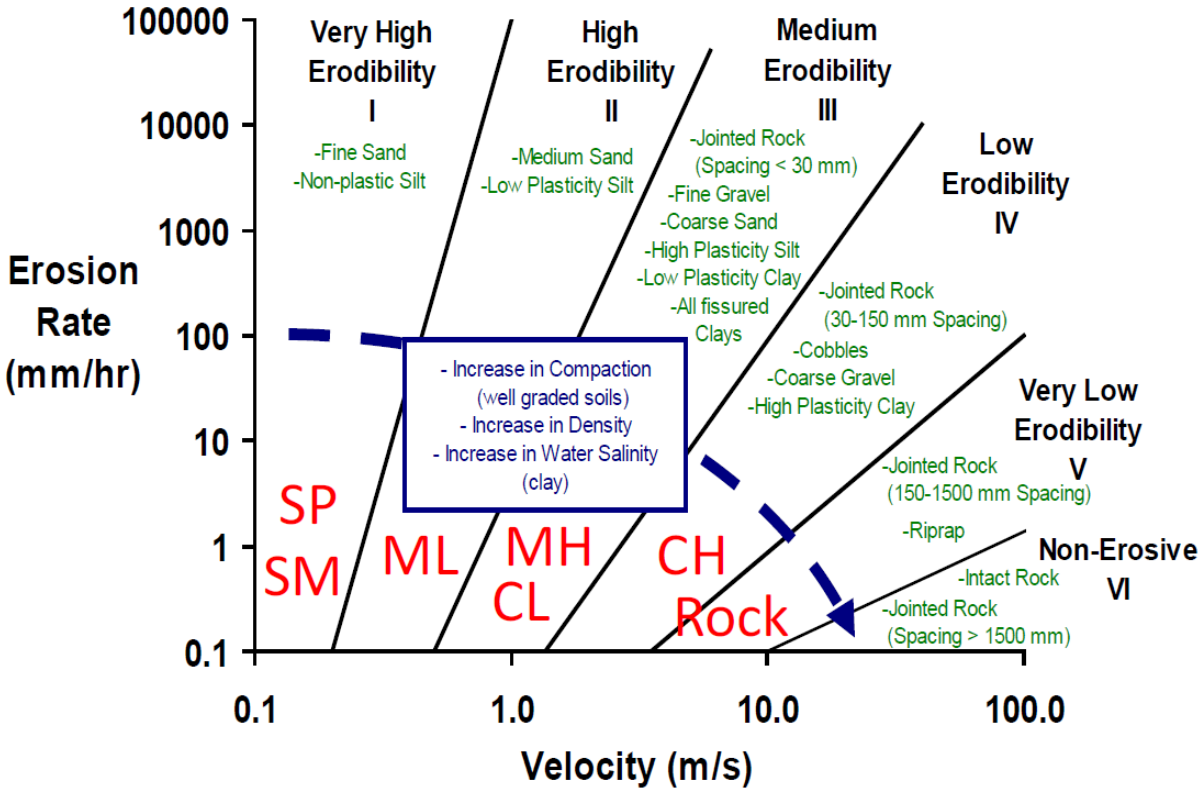

Similarly to contraction scour, maximum pier scour may not be reached during a flood or even over the life of the bridge. Therefore, the scour expected over the life of a bridge may need to account for time dependency.

The method for computing time-dependent contraction scour in cohesive materials as discussed in Section 5.4.6 of Austroads (2018) also applies to pier scour. Equations 38 to 40 from Austroads (2018) can be used to calculate incremental scour for a time series of flows expected for the life of the bridge (including extreme design events). However, the initial rate of scour and the ultimate scour must be determined for each flow condition in the subject time series of flows.

Ultimate scour is determined using Equation 5.4.10.3 while the initial rate of scour can be determined from either material testing, from Figure 5.23 of Austroads, 2018 (from shear stress) or from Figure 5.4.10.3(b) (from velocity). If using these figures; the shear stress or velocity at the pier must however, be increased to account for flow acceleration and increased turbulence.

Briaud (2011) and HEC-23 (Lagasse et al. 2009) provide equations for estimating maximum shear stress at a pier. The HEC-23 equation is reproduced below:

$$\tau_{pier} = \frac{\gamma}{y_1^{0.333}}\left(\frac{nKV_1}{K_u}\right)^2$$ Equation 5.4.10.4

Where:

τ_{pier} = shear stress at the pier, (N/m²)

γ = Unit weight of water, (N/m³)

n = Manning's n of channel bed ($m^{1/3}/s$)

y_1 = Depth of flow at pier (m)

V_1 = Approach flow Velocity

K = Velocity coefficient, 1.5 for circular piers and 1.7 for square piers

K_u = 1.0, (SI)

Section 7.12 of Arneson et al. (2012) presents an example application to calculate scour for piers in cohesive materials.

The Hydraulic Toolbox software developed by the United States of America Federal Highway Administration (FHWA, 2017) calculates the ultimate pier scour and the scour depth after a flow event of a given duration in cohesive materials based on Equation 5.4.10.3 developed by Briaud et al. (2011) and documented in Section 7.12 of Arneson et al. (2012). For most bridge pier applications, these two scour depths (ultimate and design flow event) are the only values required.

The parameters required for estimating pier scour in cohesive material with this software are the flow characteristics at the pier (depth and velocity), pier geometric characteristics (shape, width and length), angle of attack, critical velocity for onset of erosion, initial erosion rate and flow duration.

The SRICOS-EFA program developed also calculates the full suite of scour depths documented in the SRICOS-EFA method (Briaud et al. 2011).

5.4.11 Pressure flow scour

Addition

Use Equation 33 and Equation 35 to calculate y_2 for live-bed and clear-water conditions respectively.

For flow conditions that do not overtop the bridge or roadway approaches, all flow is through the bridge and the live-bed and clear-water equations can be applied directly.

When flow overtops the bridge or approach roadway, the value of Q_2 (flow in the contracted channel) in the live-bed equation (Equation 33) or Q (discharge through the bridge) in the clear-water equation (Equation 35) should include only the flow through the bridge opening. This discharge can be obtained from hydraulic model results.

For live-bed applications, the upstream channel discharge Q_1 and channel flow depth y_1 used in Equation 33 may also need adjustment. For non-overtopping flows, Q_1 is not adjusted and $y_1 = h_{ue} = h_u$. For overtopping flows, Q_1 is adjusted and $y_1 = h_{ue} = h_b + T$, where T is the height of the obstruction including girders, deck, and parapet.

If the bridge consists of railing with openings, the blockage height T extends up to the lower edge of the opening under the railing. The potential for debris blocking openings in the railing should be considered when determining T.

For overtopping flows in live-bed conditions, Q_{ue} is used instead of Q_1 in Equation 33 and can be calculated from the total channel discharge at the approach Q_1, from:

$$Q_{ue} = Q_1 \left(\frac{h_{ue}}{h_u}\right)^{8/7} \qquad \text{Equation 5.4.11(a)}$$

Where:

Q_{ue} = Effective channel discharge for live-bed conditions and bridge overtopping flow (m^3/s)

Q_1 = Upstream channel discharge as defined for Equation 33 (m^3/s)

h_u = Upstream channel flow depth as defined for Equation 33 (m)

h_{ue} = Effective upstream channel flow depth for live bed conditions and bridge overtopping (m)

It should be noted that there is no sufficient experimental data to determine the maximum thickness of the separated flow zone (t). Equation 46 was formulated based on dimensional analysis and CFD testing as a guide and then calibrated using the pressure flow scour data from Arneson (1998), TRB (1998b), Umbrell et al. (1998), and the Turner-Fairbank Highway Research Center (FHWA 2012c).

A design safety factor was applied to the constant factor, and exponents were rounded to obtain a conservative estimate of separation zone thickness (t). Therefore, using Equation 46 results in t values larger than those measured in the laboratory.

The use of Equations 33 or 35 in combination with Equation 45 incorporates the constriction of the channel and floodplain flows (lateral contraction) and pressure flow (vertical contraction). Pressure flow scour can occur even when there is no lateral contraction due to vertical contraction of the flow and the development of the flow separation zone. Note that pressure flow scour depths are calculated by implicitly using the lateral contraction equations, as such, pressure flow and lateral contraction scour depths should not be added.

Alternative methods to calculate pressure flow scour are presented in Lyn (2008) and Melville (2014). Lyn (2008) found that Equation 45 exhibits unsatisfactory behaviour due to an ill-chosen original model equation. He also found that its predictive performance was inferior to other models (over and under predicting at different conditions). Consequently, he proposed the below design equation for clear-water conditions in bridges without piers:

$$\frac{Y_s}{Y_1} = min\left[0.105\left(\frac{V_a}{V_c}\right)^{2.95}, 0.5\right] \qquad \text{Equation 5.4.11(b)}$$

Where:

Y_s is the ultimate scour depth (m)

Y_1 is the non-overtopping upstream depth (up to stagnation stream line) (m)

V_a is the initial (prior to scour velocity through bridge opening (m/s)

V_c is the critical velocity associated with incipient sediment motion (m/s)

Melville (2014) presents an equation that can be used to calculate maximum likely pressure flow scour depths for design purposes. He notes that factors can be added to this equation to account for the effect of h_b/y and possibly other effects for pressure flow scour depth; however further research is required. Recent studies suggest that Y_s/Y reduces from 0.45 to about 0.23 when h_b/y is 0.75 (B. Melville, personal communication, November 2018)

$$\frac{Y_s}{Y} = 0.75\left(\frac{V}{V_c} - 0.4\right) \quad 0.4 < \frac{V}{V_c} < 1 \quad and \quad \frac{Y_s}{Y} = 0.45 \quad 1 < \frac{V}{V_c} < 2.5 \qquad \text{Equation 5.4.11(c)}$$

Where:

Y_s is the ultimate scour depth (m)

Y is the upstream depth (including overtopping) (m)

V is the initial velocity (prior to scour velocity through bridge opening (m/s), and

V_c is the critical velocity associated with incipient sediment motion (m/s).

While not the only ones, the equations recommended to conduct a scour assessment are summarized below.

Table 5.4.11 – Equations recommended to conduct a scour assessment

Process	Recommended Methodology	Alternative methodologies
Natural / general scour	Equations 5.4.2.1(a) to 5.4.2.3	River geomorphologist advice recommended
Contraction	Equation 33, Austroads 2018 (live-bed) and Equation 35 Austroads, 2018 (clear-water)	Equation 36 (Austroads, 2018) for cohesive soils
Pressure flow (vertical contraction), for cases where water reaches the bridge deck	Equation 45 and 46 (Austroads, 2018)	Equation 5.4.11(c) can be used as alternative / verification
Pier	Equation 42 and 43 (Austroads, 2018)	A rule of thumb for maximum scour for round piers aligned with the flow, Ys= 2.4a for Froude numbers smaller than 0.8 or Ys = 3.0a for Froude numbers larger than 0.8 where a is the pier diameter can be used for verification (Melville and Coleman, 2000, Austroads, 2018). Equation 5.4.10.1 can be used as alternative. This equation is recommended for non-uniform circular piers founded on larger circular caissons. FDOT methodology is recommended for wide and complex pier foundations as described in Section 5.4.10.3. Equation 5.4.10.3 is recommended for pier scour in cohesive materials.
Abutment	Equation 5.4.9(a) and 5.4.9(b)	Velocity and unit discharge for abutment scour calculation should be derived from two-dimensional modelling. These equations predict total scour at the abutment and no contraction scour should be added to these values. A minimum of 2 m scour depth measured from the bottom of the headstock is required in accordance with *Design Criteria for bridge and other structures* (Transport and Main Roads, March 2017).

5.4.12 Worked examples

Addition

Bridge over North Kariboe Creek on Burnett Highway

An existing 28 m long timber bridge spanning North Kariboe Creek near Thangool in the Fitzroy District, Central Queensland is proposed to be replaced with a new, online, 45 m long, evenly spaced three span bridge with 1:1.5 spill-through abutments.

The proposed bridge will have a minimum deck level of 223.1 mAHD with a 0.65 m deep superstructure, a 0.37 m deep kerb and a 3% deck superelevation on the upstream side (refer to Figure 5.4.12(a). It will comprise 0.9 m diameter circular piers aligned with the flow and founded on pile caps sitting into 0.55 m octagonal piles driven to a minimum of RL of 197 mAHD. Abutments will be supported on 0.55 m octagonal piles driven to a minimum RL of 199 mAHD.

North Kariboe Creek has an incised main channel able to carry flows of about 1% AEP event magnitude without spilling in the surrounding floodplain. The bridge crossing is located about 400 m upstream of a slightly larger creek and has a uniform geometry upstream and downstream of the bridge site (refer to Figure 5.4.12(b).

The catchment draining through the bridge has an approximate area of 153 km². The bridge is not affected by backwater from the downstream creek during regional flood events. A large flood event equivalent to that of the 1% AEP event was experienced at the bridge site in 2015.

Bore logs showed a layer of medium dense and loose clayey sand (0 m to 3.5 m thick) overlaying gravel. Upper layer soil parameters were interpreted to be d_{50} = 0.6 mm and d_{95} = 2 mm.

The proposed bridge is designed for a 1% AEP local flood immunity and will only be overtopped during the 0.05% AEP local event. The 1% AEP local event was used as Serviceability Limit State (SLS) while the 0.05% AEP local flood event corresponded to the Ultimate Limit State (ULS).

Hydraulic characteristics were extracted from a two-dimensional hydrodynamic model built to inform the design. Figure 5.4.12(b) shows unit discharge and velocities at the vicinity of the bridge during the 1% AEP event. This gives an idea of the main channel and floodplain fringe conveyance and material transport potential, with the latter having shallow and slow-moving flows characterised by low values.

During the 1% AEP event, most flow is contained within the channel and slight contraction is likely to occur during this event. Hydraulic properties at the bridge for SLS and ULS are listed in Table 5.4.12(a).

Table 5.4.12(a) – Hydraulic characteristics at North Kariboe Creek Bridge

Location	Event	Flow (m^3/s)	Water Level (mAHD)	Average depth of flow (m)	Peak Velocity (m/s)	Mean velocity (m/s)
Upstream of bridge	1% AEP (SLS)	621	222.6	5.6	3.9	3.3
	0.05% AEP (ULS)	710	223.9	6.9	3.9	3.5
At bridge	1% AEP (SLS)	621	222.6	5.6	3.9	3.3
	0.05% AEP (ULS)	710	223.9	6.9	3.9	3.5

Note that required hydraulic characteristics (Q_1, Y_1, V_1 and W_1) were extracted from high conveyance areas, as ineffective flow areas upstream of bridge are unlikely to transport sediment and significantly contribute to contraction scour.

Figure 5.4.12(a) – General Arrangement, proposed North Kariboe Creek Bridge

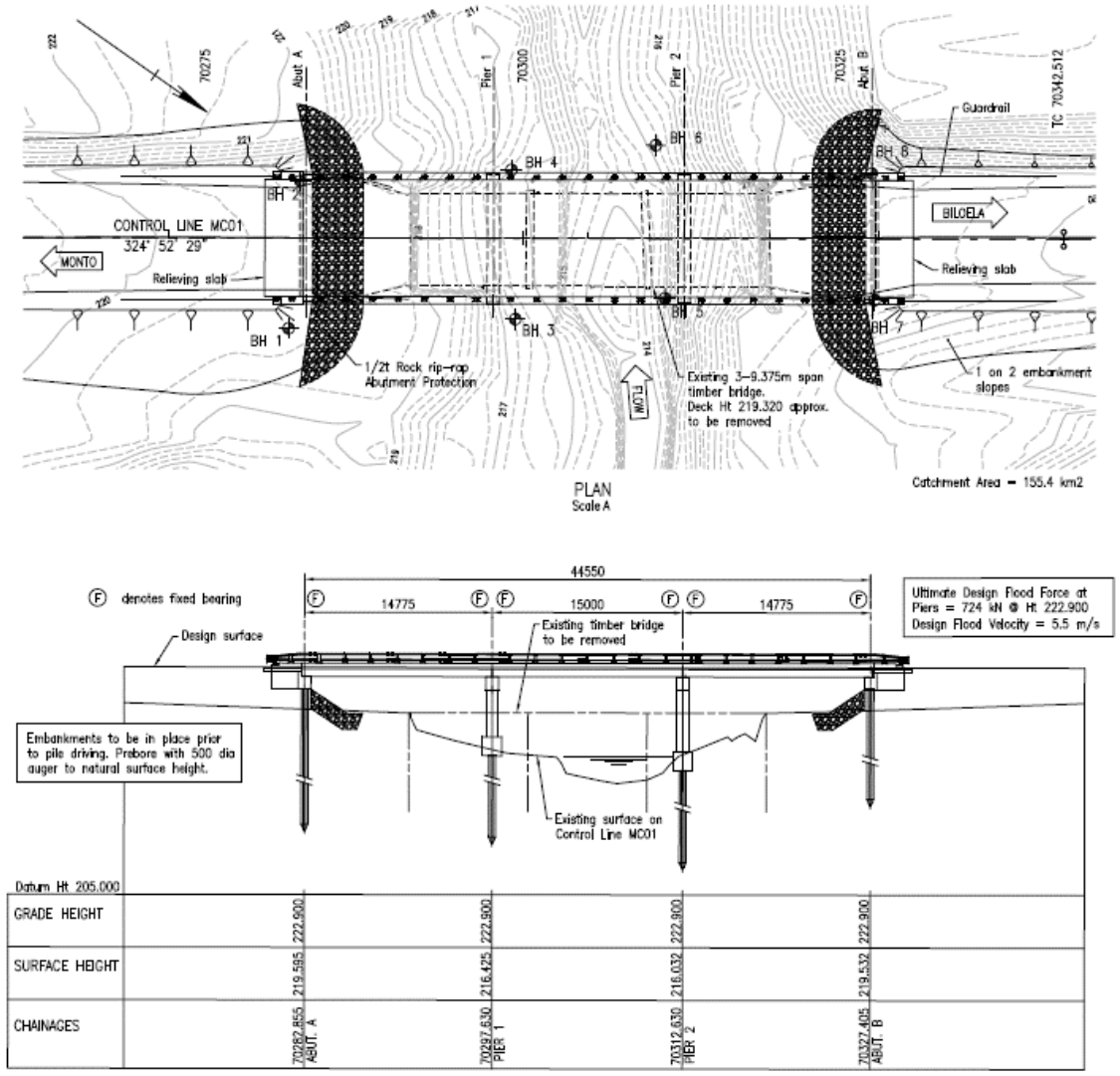

(Drawing used with permission of Transport and Main Roads Fitzroy Region).

Figure 5.4.12(b) – 1% AEP unit discharge (m²/s) and velocity vectors at proposed North Kariboe Creek Bridge

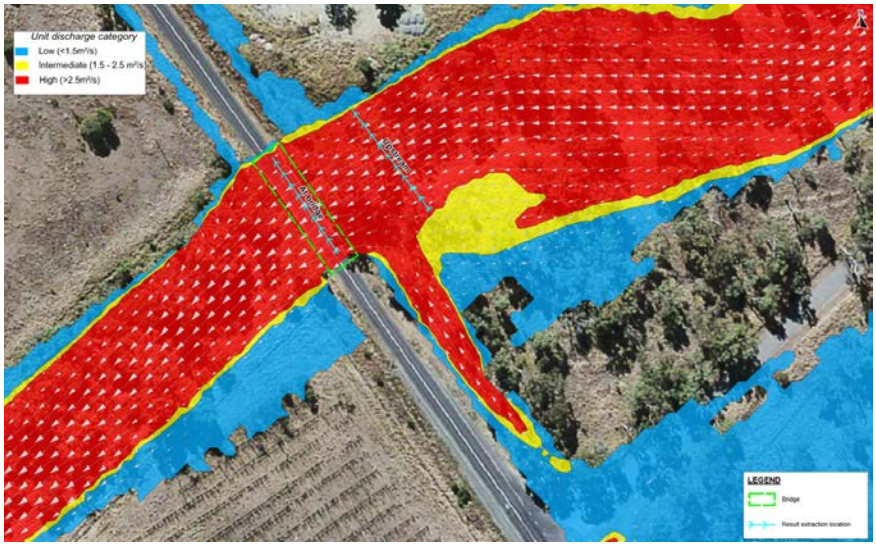

Figure adapted from (TMR, 2018c).

Step 1: Long-term bed elevation changes

Slight local degradation of the stream bed was observed under the existing bridge site after the 2015 flood event, particularly at the spill-through abutments and around the pier but the channel upstream and downstream of the bridge appeared to be relatively stable with well-vegetated banks (see Figure 5.4.12(c). Consequently, no natural scour is considered for this bridge.

Figure 5.4.12(c) – Existing North Kariboe Creek Bridge (looking downstream)

Step 2: Estimate magnitude of contraction scour

a) For the 1% AEP (SLS) flood event

As the overbank flow is mostly obstructed by the road embankment and no contraction of the channel occurs, the bridge is considered Case 1b regarding contraction (see Section 5.2.7, Austroads 2018). From Equation 5.4.3(a), V_c = 0.69 for the bed underlying material. Consequently, live bed conditions will occur at this bridge during this event. The shear velocity in the upstream section is V* = 0.57 m/s (from Table 5.1, Austroads 2018). Assuming a temperature of 18°, the fall velocity of bed material (ω) is 0.08 m/s (from Figure 5.20, Austroads 2018), thus k_1 = 0.69 (mostly suspended bed material).

Q_1	Q_2	y_1	V_1	Fr_1	S_1	W_1	W_2	y_2	y_s
(m^3/s)	(m^3/s)	(m)	(m/s)		(m/m)	(m)	(m)	(m)	(m)
621	621	5.6	3.3	0.44	0.006	45	43.2	5.76 (Eq. 33, Austroads, 2018)	0.16 (Eq. 34, Austroads, 2018)

$Q_1 = Q_2$ as flow is contained within main channel and hardly any contraction occurs, W2 = 43.2 m (excluding pier widths).

As the water depth just reaches the upstream side of the deck, pressure flow scour is also considered.

h_u	T	h_b	h_t	h_w	t	y_s
(m)	(m)	(m)	(m)	(m)	(m)	(m)
5.6	1.0m*	5.4	0.2	0	1.4 (Eq. 46, Austroads, 2018)	1.7 (Eq. 45, Austroads, 2018)

*T = 1.0 m = 0.65 m deck+0.37 m kerb, $h_{ue} = h_u$ =y1 = 5.6 m and hw = 0 as bridge is not overtopped during this event (refer to Figure 5.4.12(d)).

b) For the 0.05% AEP (ULS) flood event the bridge is overtopped

From Equation 5.4.3(a) V_c = 0.72. Live bed conditions will also occur at this bridge during this event. V* = 0.45, ω = 0.08 m/s and k_1 = 0.69.

Q_1	Q_2	y_1	V_1	Fr_1	S_1	W_1	W_2	y_2	y_s
(m^3/s)	(m^3/s)	(m)	(m/s)		(m/m)	(m)	(m)	(m)	(m)
710	710	6.9	3.5	0.43	0.003	45	43.2	7.1 (Eq. 33, Austroads, 2018)	0.2 (Eq. 34, Austroads, 2018)

As the water depth overtops the deck, pressure flow scour is also considered.

h_u	h_{ue}	T	h_b	h_t	h_w	t	y_s
(m)	(m)	(m)	(m)	(m)	(m)	(m)	(m)
6.9	6.4	1.0 m*	5.4	1.5	0.5	2.0 (Eq. 46, Austroads, 2018)	3.6 (Eq. 45, Austroads, 2018)

*T = 1.0 m = 0.65 m deck + 0.37 m kerb of superelevation, as bridge is overtopped during this event, refer to Figure 5.4.12(d) for variable definition.

Note that pressure flow (vertical contraction) scour depths are considerably larger than lateral contraction scour depths. As such, calculated pressure flow scour values (1.7 m and 3.6 m) are used to account for contraction scour in both SLS and ULS events. Although, not strictly applicable ($V/V_c > 2.5$), resulting values are consistent with those obtained with Equation 5.4.11(c) which predicts 2.5 m and 3 m pressure flow scour depths for the SLS and ULS events respectively.

Figure 5.4.12(d) – Pressure flow variables – Proposed North Kariboe Creek Bridge

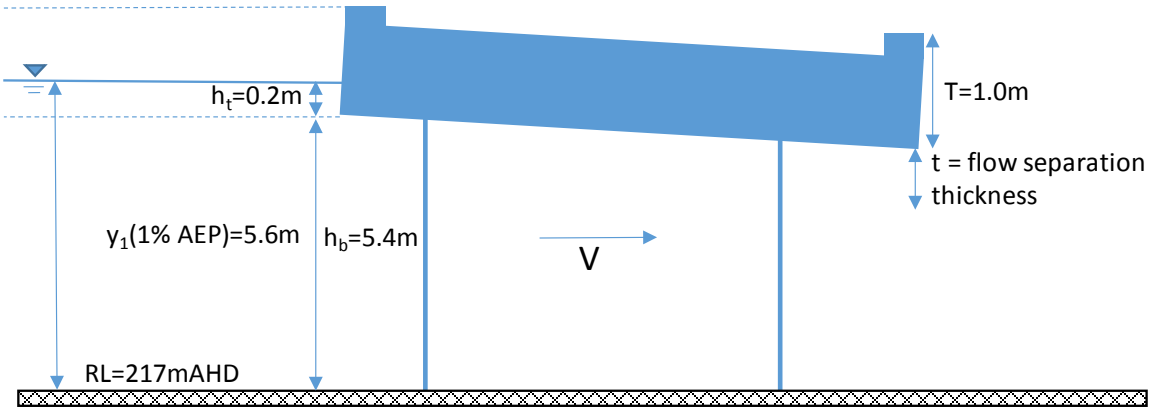

a) 1% AEP (SLS)

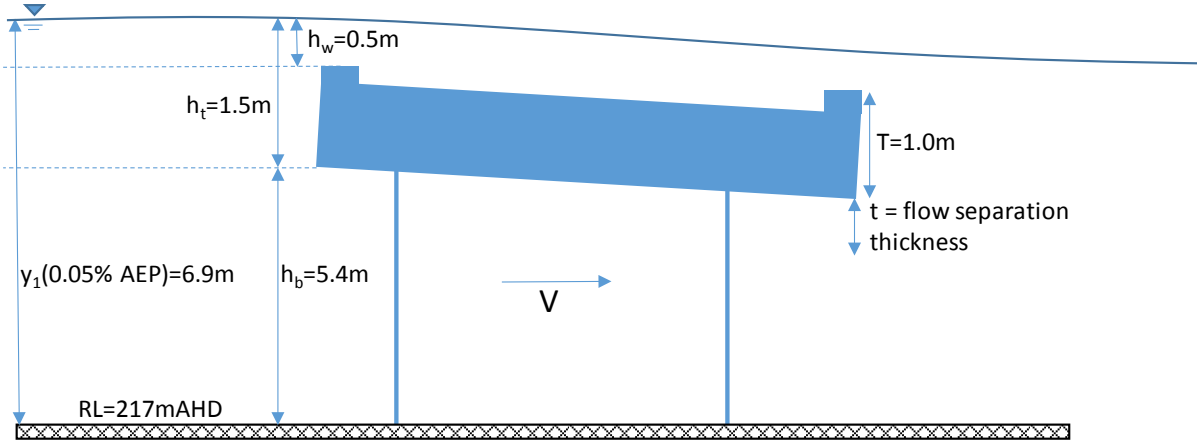

c) 0.05% AEP (ULS)

Step 3: Estimate magnitude of local pier scour

a) For the 1% AEP (SLS) flood event

y_1	V_1	Fr_1	K_1	K_2	K_3	y_s
(m)	**(m/s)**					**(m)**
5.6	3.3	0.44	1 (cylindrical)	1 (θ=0^o)	1.1 (plane bed)	2.7 (Eq. 42, Austroads, 2018)

b) For the 0.05% AEP (ULS) flood event the bridge is overtopped

y_1	V_1	Fr_1	K_1	K_2	K_3	y_s
(m)	**(m/s)**					**(m)**
6.9	3.5	0.43	1 (cylindrical)	1 (θ=0^o)	1.1 (plane bed)	2.8 (Eq. 42, Austroads, 2018)

These values are consistent with those obtained using the rule of thumb for maximum scour for round piers aligned with the flow (Melville and Coleman, 2000, Austroads, 2018), Ys= 2.4a = 2.2 m, where a is the pier diameter.

As the piers are founded on 1.5 m high, 1.5 m wide, 6 m long pile caps setting just below the bed stream, the pile cap scour was also computed following the procedure for complex piers (Case 2) documented on Section 7.5 of Arneson et al. (2012) (refer to Section 5.4.10.3).

Only calculations for Pier 2 (worst case scenario) are herein documented. The total values calculated including pier and pilecap scour are therefore adopted.

c) For the 1% AEP (SLS) flood event

a	a_{pc}	T	h_0	h_1	K_1	K_2	K_3	K_{ph}	$Y_{s(pier)}$	h_2	y_2	v_2	K_s	y_f	V_f
(m)	**(m)**	**(m)**	**(m)**	**(m)**					**(m)**	**(m)**	**(m)**	**(m)**	**(m)**	**(m)**	**(m/s)**
0.9	1.5	1.5	-1.5	0	1	1	1.1	0.31	0.85	-1.1	6.0	3.1	0.001	0.41	2.33
$Y_{spilecap}$	Y_{total}														
(m)	(m)														
2.25	3.10														

Refer to Section 7.5 of Arneson et al. (2012) and Section 5.4.10.3

d) For the 0.05% AEP (ULS) flood event

a	a_{pc}	T	h_0	h_1	K_1	K_2	K_3	K_{ph}	$y_{s(pier)}$	h_2	y_2	V_2	K_s	y_f	V_f
(m)	**(m)**	**(m)**	**(m)**	**(m)**					**(m)**	**(m)**	**(m)**	**(m)**	**(m)**	**(m)**	**(m/s)**
0.9	1.5	1.5	-1.5	0	1	1	1.1	0.31	0.87	-1.1	7.2	3.3	0.001	0.44	2.47
$Y_{spilecap}$	Y_{total}														
(m)	(m)														
2.30	3.20														

Refer to Section 7.5 of Arneson et al. (2012) and Section 5.4.10.3

Step 4: Estimate magnitude of local abutment scour

a) For the 1% AEP (SLS) flood event

Abutment	y_a	V_1	Fr_1	L'	K_1	K_2	y_s
	(m)	(m/s)		(m)			(m)
A (south)	2.35	2.6	0.54	2	0.55 (spill through)	1.0 (θ=90°)	4.2 (Eq. 41, Austroads, 2018)
B (north)	2.50	1.2	0.24	2	0.55 (spill through)	1.0 (θ=90°)	3.7 (Eq. 41, Austroads, 2018)

Note that the Y_a, V_1 and L' values were derived from 2D model results (see Figure 5.4.12(b).

Due to the uncertainty of the L' values estimated, the NCHRP 24-20 method is also used to calculate local abutment scour. Note that the spill through abutments are set near the channel such that L/Bf = 0.9.

Abutment	y_1	y_0	q_{2c}	q_1	y_c	αa	y_{max}	y_s
	(m)	(m)	(m^2/s)	(m^2/s)	(m)		(m)	(m)
A and B	5.6	5.6	14.4*	13.8*	5.8 Eq. 5.4.9(c)	1.4 (spill through / live bed)	8.1 Eq. 5.4.9 (a)	2.5 Eq. 5.4.9(b)

*Values were derived from 2D model results (see Figure 5.4.10(b)).

b) For the 0.05% AEP (ULS) flood event the bridge is overtopped.

Abutment	y_a	V_1	Fr_1	L'	K_1	K_2	y_s
	(m)	(m/s)		(m)			(m)
A (south)	3.8	2.2	0.36	2	0.55 (spill through)	1.0 (θ=90°)	5.7 (Eq. 41, Austroads, 2018)
B (north)	3.6	3.9	0.66	2	0.55 (spill through)	1.0 (θ=90°)	6.3 (Eq. 41, Austroads, 2018)

Note that the Y_a, Q_e, Ae, V_1 and L' values were derived from 2D model results (see Figure 5.4.10(b)).

Due to the uncertainty of the L' values, the NCHRP 24-20 method is used to calculate abutment scour.

Abutment	y_1	y_0	q_{2c}	q_1	y_c	α_a	y_{max}	y_s
	(m)	(m)	(m^2/s)	(m^2/s)	(m)		(m)	(m)
A and B	6.4*	6.4*	16.4	15.8	6.6 Eq. 5.4.9(c)	1.4 (spill through / live bed)	9.2 Eq. 5.4.9(a)	2.8 Eq. 5.4.9(b)

Values derived from 2D model results (see Figure 5.4.12(b)), *maximum water depth before overtopping used.

These values are consistent with those obtained for pressure flow, consequently NCHRP 24-20 values (2.5 m and 2.8 m) are adopted to account for scour at abutments, as the NCHRP 24-20 equations predict total scour at the abutment no contraction scour is added to these values.

Note that the NCHRP 24-20 method does not provide guidance about how to incorporate pressure scour using this approach. Given that the subject channel is relatively side (W = 45m), it is assumed that the pressure scour occurs in the middle section of the bridge opening, away from the abutments. As adding pressure flow and abutment scour will yield very conservative (unrealistic) scour depths,

this method is recommended. However, this approach may not be appropriate for narrow crossings where pressure scour might occur across the entire bridge opening.

Step 5: Plot total scour depths and evaluate foundation design

Scour depths calculated at piers and abutments are listed in the below table. Note that total scour depths at piers are the sum of contraction and pier calculated depths while abutment scour depths do not include contraction scour (as recommended by NCHRP 24-20).

Design Event	Pressure Scour	Pier Scour	Abutment Scour	Total Pier Scour	Total Abutment Scour
(AEP)	(m)	(m)	(m)	(m)	(m)
1% (SLS)	1.7	3.1	2.5	**4.8**	**2.5**
0.05% (ULS)	3.6	3.2	2.8	**6.8**	**2.8**

RL's of total scour depths (in mAHD) at piers and abutments are listed in the table below and plotted on Figure 5.4.12(e) alongside the geotechnical limits estimated from borehole logs by a geotechnical engineer based on type of soil and Standard Penetration Test values (SPTs). Note that predicted scour depths would be limited by the top of the gravel layer. The scour levels ultimately adopted for bridge design during the ULS event are highlighted in the below table and figure.

Location	Ground Level	1% AEP Total Scour RL	0.05% AEP Total Scour RL	Geotechnical Threshold RL	Scour levels adopted for SLS (1% AEP)	Scour levels adopted for ULS (0.05% AEP)
	(mAHD)	(mAHD)	(mAHD)	(mAHD)	(m)	(mAHD)
Abutment A	221.1/219.6*	217.1	216.8	209.1	**217.1**	**216.8**
Pier 1	216.4	211.6	209.6	210.2	**211.6**	**210.2**
Pier 2	216.0	211.2	209.2	208.0	**211.2**	**209.2**
Abutment B	221.1/219.6*	217.1	216.8	219.3	**219.3**	**219.1****

*Denotes abutment headstock/surface levels at centreline, **a minimum of 2 m scour depth measured from the bottom of the headstock is required for ULS design in accordance with *Design Criteria for Bridge and Other Structures* (Transport and Main Roads, March 2017).

Figure 5.4.12(e) – Calculated scour depths vs. geotechnical threshold at North Kariboe Creek Bridge

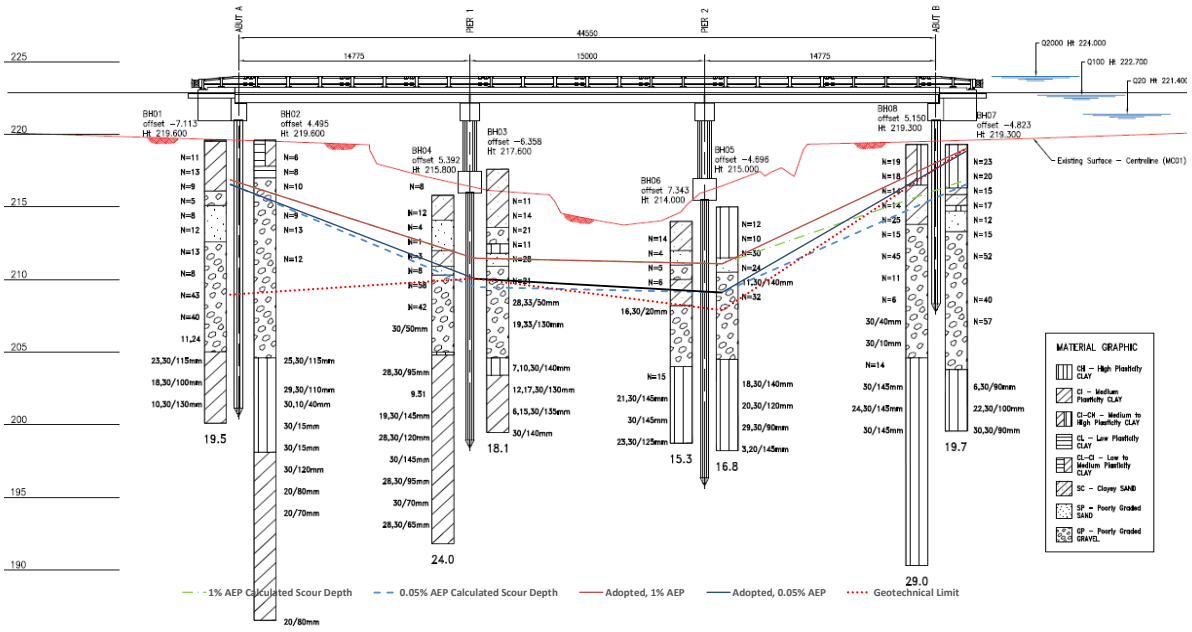

Step 6: Determine protection required at abutments

Abutments were designed to provide protection against scour up to the 1% AEP event. The recommended abutment protection was sized based on the Austroads 1994 method (using the maximum velocity instead of the factored mean velocity), for a given velocity of 3.9 m/s and spill through abutment slopes of 1V:1.5H, this consists of 1.25 m thick, ½ tonne riprap (d_{50} = 700 mm) including a self-launching toe to armour abutments and reduce the risk of scour. If the factored mean velocity at the bridge is used, rock class would increase to 1 tonne rock (d_{50} = 1000 mm). Ultimately, the chosen solution was selected using engineering judgement based on hydraulic, structural, material and construction merits. Details of the rock class are given in Table 5.12 of Austroads 2018.

Bridge over Doubtful Creek on Dawson Highway

An existing 36.5 m long timber bridge spanning Doubtful Creek near Voewood in the Fitzroy Region, Central Queensland is to be replaced with a new, online, 56.5 m long, evenly spaced three span bridge with 1:1.5 spill-through abutments (refer to Figure 5.4.12(f)). The proposed bridge will be on grade and have a minimum deck level of 70.74 mAHD with a 0.85 m deep superstructure, a 0.37 m deep kerb and a 3% deck superelevation on the upstream side. It will comprise 1.2 m diameter cast in-situ circular piles aligned with the flow at a minimum RL of 50 mAHD. Abutments will be supported on 1.2 m diameter circular piles cast in-situ at 56.5 mAHD RL.

Doubtful Creek has an incised main channel able to carry flows of about 1% AEP event magnitude without spilling in the surrounding floodplain. The bridge crossing is located about 3 km upstream of the larger Calliope River and has a fairly uniform geometry upstream and downstream of the bridge site (refer to Figure 5.4.12(g)). A large flood event equivalent to that of the 1% AEP event was experienced at the bridge site in 2015.

The catchment draining through the bridge has an approximate area of 33.6 km². The bridge is not affected by backwater from Calliope River during regional flood events. Bore logs showed a layer of alluvium and sandy clay (2 m to 3 m thick) overlaying granodiorite bedrock. Upper layer soil parameters were interpreted to be d_{50} = 0.2 mm and d_{95} = 2 mm.

The proposed bridge is designed for a 1% AEP regional flood immunity but will not be overtopped even during the 0.05% AEP local event. The 1% AEP local event was used as Serviceability Limit State (SLS) while the 0.05% AEP local flood event corresponded to the Ultimate Limit State (ULS).

Hydraulic characteristics were extracted from a two-dimensional hydrodynamic model built to inform the replacement. Figure 5.4.12(g) shows unit discharge and velocities at the vicinity of the bridge during the 1% AEP event. This gives an idea of the main channel and floodplain fringe conveyance and material transport potential, with shallow and slow-moving flows characterised by low values. Hydraulic properties at the bridge for SLS and ULS are listed in Table 5.4.12(b).

Table 5.4.12(b) – Hydraulic characteristics at Doubtful Creek Bridge

Location	Event	Flow	Water Level	Average depth of flow	Peak Velocity	Mean velocity
		(m^3/s)	(mAHD)	(m)	(m/s)	(m/s)
Upstream of bridge	1% AEP (SLS)	340	70.2	3.5	3.0	2.0
	0.05% AEP (ULS)	605	71.5	4.8	3.6	2.7
At bridge	1% AEP (SLS)	340	70.2	3.5	2.8	2.0
	0.05% AEP (ULS)	605	71.5	4.8	3.4	3.0

Figure 5.4.12(f) –Doubtful Creek Bridge Replacement – General Arrangement

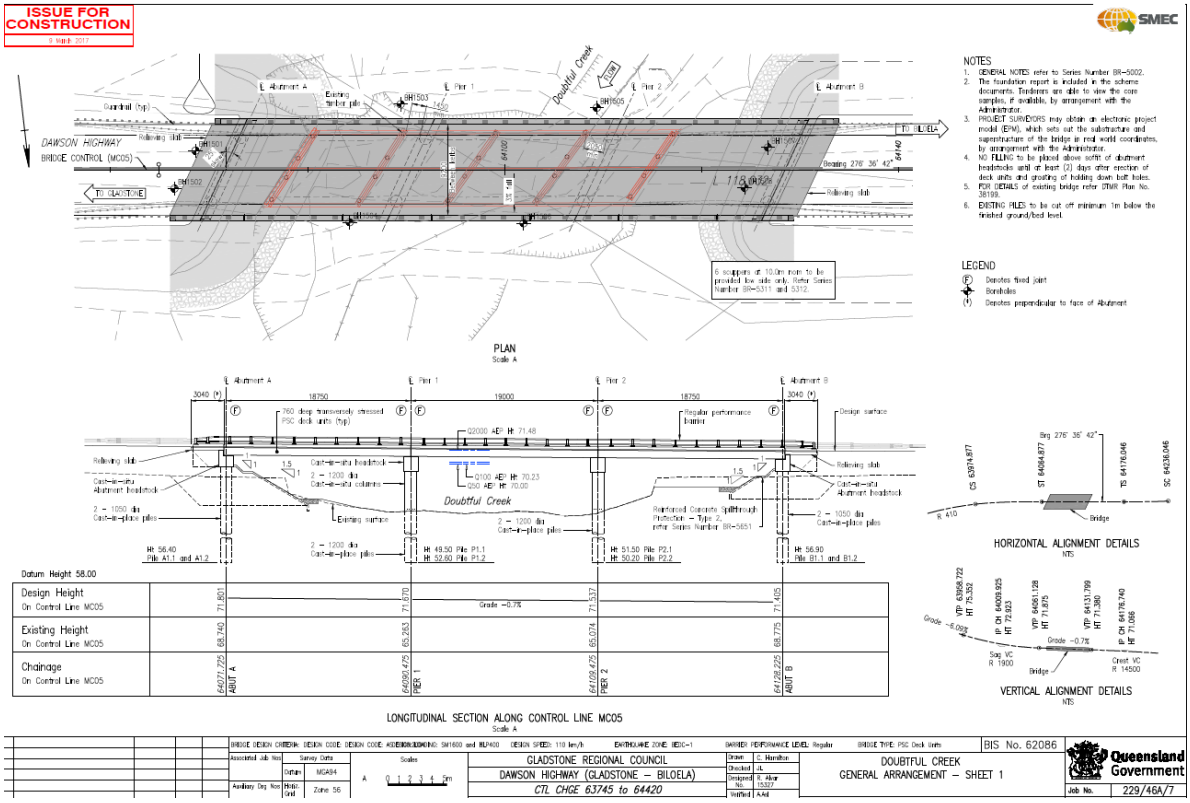

(Drawing used with permission of SMEC and Transport and Main Roads Fitzroy Region).

Figure 5.4.12(g) – 1% AEP unit discharge (m^2/s) and velocity vectors at Doubtful Creek Bridge

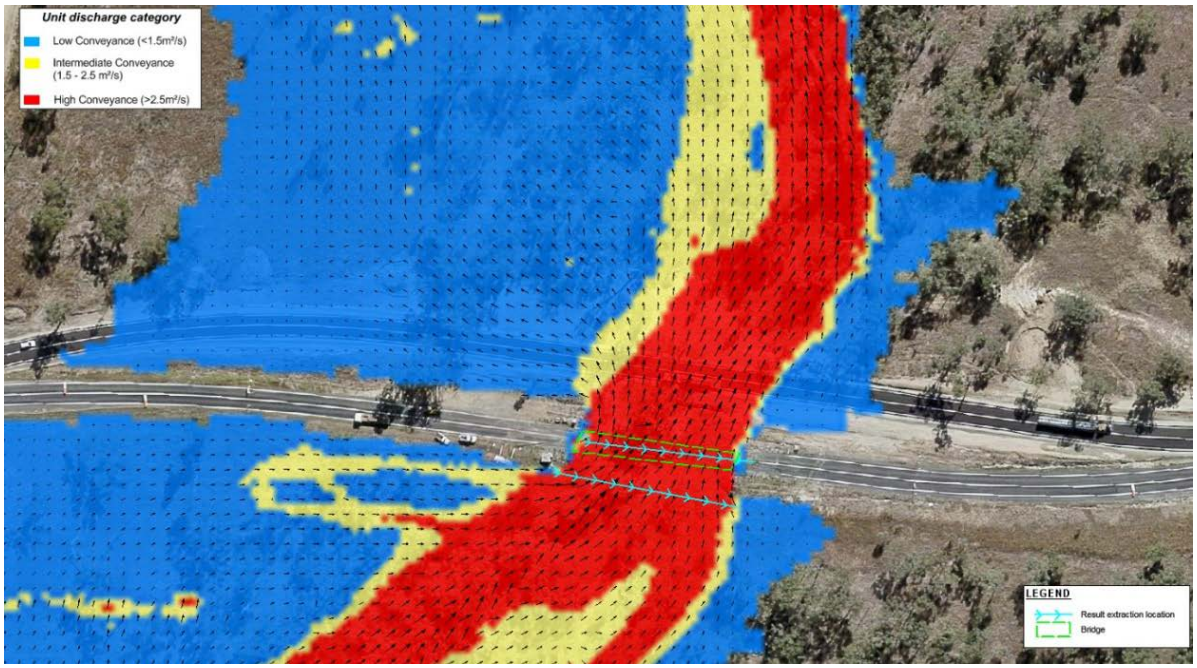

Figure adapted from (SMEC, 2016).

Figure 5.4.12(h) – Existing Doubtful Creek Bridge (looking downstream)

Step 1 – Natural scour

Although some evidence of localised scour at the existing bridge was noted after the 2015 event (see Figure 5.4.12(h)), the channel is relatively stable with well-vegetated banks. As the 2015 flood events did not cause any change in the alignment of the stream channel, no natural scour was accounted for.

Step 2: Estimate magnitude of contraction scour

a) For the 1% AEP (SLS) flood event

As the overbank flow is mostly obstructed by the road embankment and only a slight contraction of the channel occurs, the bridge is considered Case 1b (see Section 5.2.7, Austroads 2018).

From Equation 5.4.3(a), $V_c = 0.45$ for the bed underlying material. Consequently, live bed conditions will occur at this bridge during this event. The shear velocity in the upstream section is V* = 0.41 m/s

(from Table 5.1, Austroads 2018). Assuming a temperature of 18°, the fall velocity of bed material (ω) is 0.022 m/s (from Figure 5.20, Austroads 2018), thus k_1 = 0.69 (mostly suspended bed material).

Q_1	Q_2	y_1	V_1	Fr_1	S_1	W_1	W_2	y_2	y_s
(m^3/s)	(m^3/s)	(m)	(m/s)		(m/m)	(m)	(m)	(m)	(m)
340	340	3.5	2.0	0.34	0.005	65	54.1	4.0 (Eq. 33, Austroads, 2018)	0.5 (Eq. 34, Austroads, 2018)

$Q_1 = Q_2$ as flow is contained within main channel and hardly any contraction occurs, W_2 = 54.1 m (excluding pier widths).

b) For the 0.05% AEP (ULS) flood event the bridge is overtopped.

From Equation 5.4.3(a) V_c = 0.47. Live bed conditions will also occur at this bridge during this event. V* = 0.49, ω = 0.08 m/s and k_1 = 0.69.

Q_1	Q_2	y_1	V_1	Fr_1	S_1	W_1	W_2	y_2	y_s
(m^3/s)	(m^3/s)	(m)	(m/s)		(m/m)	(m)	(m)	(m)	(m)
605	605	4.8	3.0	0.44	0.005	65	54.1	5.4 (Eq. 33, Austroads, 2018)	0.6 (Eq. 34, Austroads, 2018)

As the water depth reaches the upstream side of the deck, pressure flow scour is also considered.

h_u	T	h_b	h_t	h_w	t	y_s
(m)	(m)	(m)	(m)	(m)	(m)	(m)
4.8	1.2 m*	3.65	1.2	0	1.3 (Eq. 46, Austroads, 2018)	3.1 (Eq. 45, Austroads, 2018)

*T = 1.2 m = 0.85 m deck+0.37 m kerb, $h_{ue} = h_u = Y_1$ = 4.7 m and h_w = 0 as bridge is not overtopped during this event (refer to Figure 5.4.12(d)).

A contraction scour of 0.5 m is accounted for the SLS event while the pressure flow scour value (3.1 m) is used to account for contraction scour in the ULS event. Although, not strictly applicable ($V/V_c > 2.5$), resulting values are consistent with those obtained with Equation 5.4.11(c) which predicts a 2.2 m pressure flow scour depth for the ULS event.

Step 3: Estimate magnitude of local pier scour

a) For the 1% AEP (SLS) flood event.

y_1	V_1	Fr_1	K_1	K_2	K_3	y_s
(m)	(m/s)					(m)
3.5	2.0	0.34	1 (cylindrical)	1 (θ=0)	1.1 (plane bed)	2.4 (Eq. 42, Austroads, 2018)

b) For the 0.05% AEP (ULS) flood event the bridge is overtopped

y_1	V_1	Fr_1	K_1	K_2	K_3	y_s
(m)	(m/s)					(m)
4.8	3.0	0.44	1 (cylindrical)	1 (θ=0)	1.1 (plane bed)	3.0 (Eq. 42, Austroads, 2018)

These values are consistent with those obtained using the rule of thumb for maximum scour for round piers aligned with the flow (Melville and Coleman, 2000, Austroads, 2018), Ys = 2.4a = 2.9 m, where a is the pier diameter.

Step 4: Estimate magnitude of local abutment scour

a) For the 1% AEP (SLS) flood event.

The NCHRP 24-20 method is used to calculate local abutment scour. Note that the spill through abutments are set near the channel such that L/Bf = 0.8.

Abutment	y_1	y_0	q_{2c}	q_1	y_c	αa	y_{max}	y_s
	(m)	(m)	(m^2/s)	(m^2/s)	(m)		(m)	(m)
A and B	3.5	3.5	6.0	5.2	4.0 Eq. 5.4.9(c)	1.65 (spill through / live bed)	6.5 Eq. 5.4.9(a)	3.0 Eq. 5.4.9(b)

*Values were derived from 2D model results (see Figure 5.4.10(b)).

b) For the 0.05% AEP (ULS) flood event the bridge is overtopped.

The NCHRP 24-20 method is also used to calculate local abutment scour.

Abutment	y_1	y_0	q_{2c}	q_1	y_c	αa	y_{max}	y_s
	(m)	(m)	(m^2/s)	(m^2/s)	(m)		(m)	(m)
A and B	4.8	4.8	10.7	9.3	5.4 Eq. 5.4.9(c)	1.65 (spill through / live bed)	8.9 Eq. 5.4.9(a)	4.0 Eq. 5.4.9(b)

Values were derived from 2D model results (see Figure 5.4.12(b)).

These values are consistent with those obtained for pressure flow, consequently NCHRP 24-20 values (3.0 m and 4.0 m) are adopted to account for scour at abutments, as the NCHRP 24-20 equations predict total scour at the abutment no contraction scour is added to these values.

As for the previous example, no pressure scour has been added to abutment scour calculations. Given that the subject channel is relatively side (W = 60 m), it is assumed that the pressure scour will occur in the middle section of the bridge opening, away from the abutments.

As adding pressure flow and abutment scour will yield very conservative (unrealistic) scour depths, this method is recommended, however this approach may not be appropriate for narrow crossings where pressure scour might occur across the entire bridge opening.

Step 5: Plot total scour depths and evaluate foundation design

Scour depths calculated at piers and abutments are listed in the below table. Note that total scour depths at piers are the sum of contraction and pier calculated depths while abutment scour depths do not include contraction scour (as recommended by NCHRP 24-20).

Design Event	Contraction / Pressure Scour	Pier Scour	Abutment Scour	Total Pier Scour	Total Abutment Scour
(AEP)	(m)	(m)	(m)	(m)	(m)
1% (SLS)	0.5	2.5	3.0	**3.0**	**3.0***
0.05% (ULS)	3.0	3.0	4.0	**6.0**	**4.0***

*Abutment scour depths were used as total scour depths at abutments.

The RL's of total scour depths calculated at piers and abutments are listed in the table below and plotted on Figure 5.4.12(e) alongside the geotechnical limits estimated from borehole logs based in type of soil and Standard Penetration Test values (SPTs) larger than 15. Predicted scour depths would be limited by the top of the granodiorite bedrock layer. The scour levels ultimately adopted for bridge design during the ULS event are highlighted in the below table and figure.

Location	Ground Level	1% AEP Total Scour RL	0.05% AEP Total Scour RL	Geotechnical Threshold RL	Scour levels adopted for SLS (1% AEP)	Scour levels adopted for ULS (0.05% AEP)
	(mAHD)	(mAHD)	(mAHD)	(mAHD)	(mAHD)	(mAHD)
Abutment A	70.9 / 69.6*	66.6	65.6	65.0	**66.6**	**65.6**
Pier 1	65.3	62.3	59.3	63.0	**63.0**	**63.0**
Pier 2	65.1	62.1	59.1	64.0	**64.0**	**64.0**
Abutment B	70.6 / 69.3*	66.3	65.3	66.0	**66.3**	**66.0**

*Denotes abutment headstock / surface levels at centreline.

Step 6: Determine protection required at abutments

Type 2 reinforced concrete spill through bridge abutments were designed for this bridge, as such, several scenarios were analysed to provide the most robust solution to protect the abutments from scour. The chosen solution consisted of 0.5 m thick, 2 m long self-launching toes wrapping around the abutments to reduce the risk of scour up to the 1% AEP event. For a given mean velocity of 2.0 m/s the recommended toe abutment protection toes consist of Facing class (d_{50} = 300 mm) riprap.

Note that the rock class for the toe was selected based on the Austroads, 1994 method (using the mean velocity but without factoring the mean velocity by 1.33).

If the factored mean velocity or the maximum velocity at the bridge are used, rock class would correspond to light rock (d_{50} = 400 mm). Ultimately, the recommended solution was chosen using engineering judgement based on hydraulic, structural, material and construction merits. Details of the rock class and rock sizes are given in Table 5.12 of Austroads, 2018.

Figure 5.4.12(j) – Estimated scour depths and geotechnical threshold at Doubtful Creek Bridge Replacement

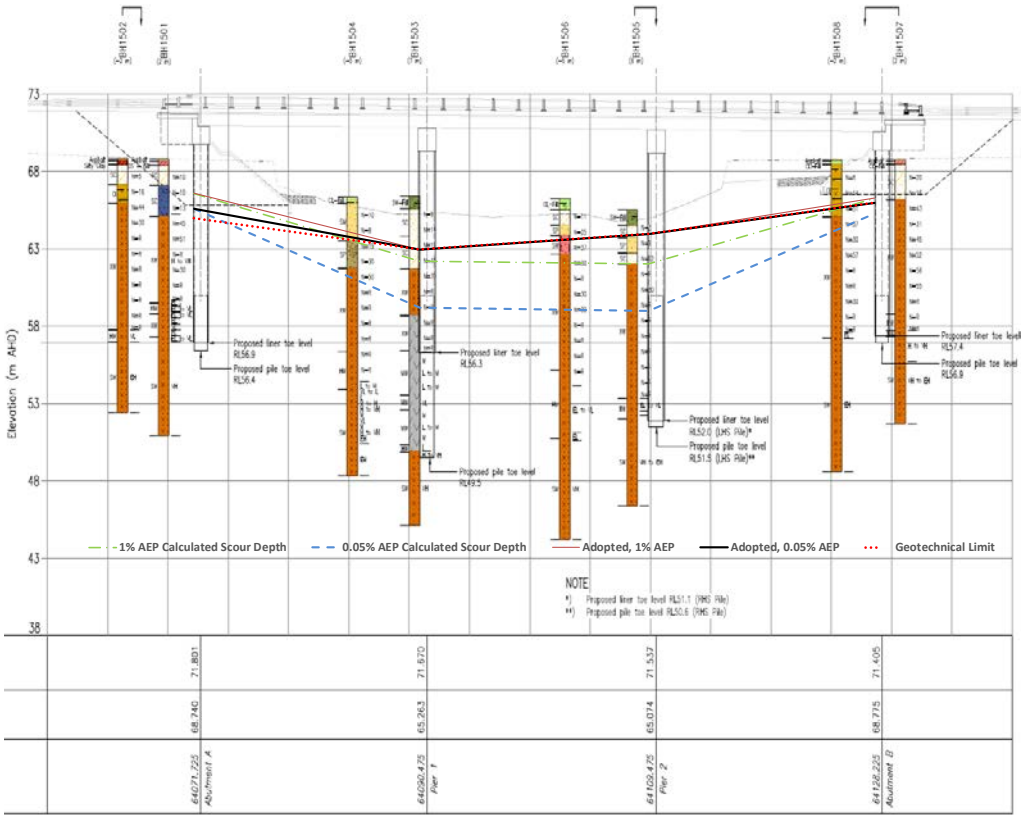

(Drawing used with permission of SMEC and Transport and Main Roads Fitzroy Region, source: SMEC, 2016).

5.5 Scour countermeasures

5.5.1 Introduction

Addition

This chapter should be read in conjunction with the MRTS03 Technical Specification (TMR 2018b), *Design Criteria for Bridges and Other Structures* (TMR 2018a) and Transport and Main Road's abutment protection Standard Drawings (2232 - 2237, 2238 and 2241). The above standards take precedence if any contradiction occurs.

Specialist advice should be sought when designing scour countermeasures, as this chapter cannot cover all the likely scenarios encountered throughout Queensland. The following guidelines do not constitute or replace specialist engineering assistance. Design advice must always be sought from an RPEQ engineer with relevant experience.

It should also be noted in accordance with (TMR 2018a), design of bridge piers for new bridges, shall not be relied on a pier scour protection. New bridges shall be designed by taking into account estimated maximum scour depth at piers to make sure structural integrity of the bridge under the action of scour. Pier scour protection is not recommended for new bridges.

Bridge abutments shall be designed by taking into consideration possible scour determined by scour analysis. Abutments shall be adequately protected to prevent scour for floods up to the SLS event. However, any scour protection designed for SLS conditions, shall not be relied upon at the ULS event (as per Clause 11.1, AS 5100.1).

5.5.2 Countermeasure groups and characteristics

Addition

Another type of armouring countermeasures are:

- concrete retaining wall mass blocks, and
- rock-filled filter bags.

5.5.3 Considerations for selecting countermeasures

Addition

Scour protection measures are designed to protect the channel bed and banks from the erosive forces causing scour. They can be categorised as flexible or rigid. Flexible systems can manage some movement without losing their armouring capability and are able to adjust to settlement or movement of the underlying and adjacent surface or bed, however they are susceptible to failure from movement of the armour material, either because it is undersized or because of loss of material at its edges. Rigid systems cannot adjust to changes in the underlying surface and are mostly impermeable. While normally more resistant to erosion, they are susceptible to failure by undermining and uplift (seepage pressure). Factors influencing the choice of scour countermeasure are outlined in Table 5.5.3.

It should be noted that experience in Queensland suggests that one of the most common causes of failure of rigid systems at abutments is undermining. As such, the use of rigid abutment protection (Type 2, Type 4 and Rock Masonry) are not recommended at bridges that experience cross-section averaged stream velocities higher than 2 m/s.

Table 5.5.3 – Selection of scour countermeasures

Scour Countermeasure	Underwater construction	Repairs	Construction cost	Maintenance cost	Restricted access	Environmental suitability	High velocity flow	Vertical stream instability	Lateral instability
Concrete mass blocks	×	✓	H	M	×	✓	✓	✓	✓
Rock-filled bags	○	✓	L	M	○	✓	✓	✓	○
Guide banks	✓	○	H	M	○	○	✓	✓	○
Cable-tied blocks	○	✓	M	M	○	✓	✓	✓	○

Notes: High – H, Moderate – M, Low – L ✓Appropriate, ○ May be appropriate, ×Inappropriate

5.5.4 Design of countermeasures

Filter layer

Addition

In general, where dune-type bedforms may be present during flood events, it is strongly recommended that only a geotextile filter be considered for use with countermeasures. Guidance for the design of both granular and geotextile filters (including examples) is provided in the Design Guide 16, Volume 2 of HEC-23 (Lagasse et al. 2009).

It should be noted that placing geotextiles under water is problematic, as most geotextiles used as filters beneath riprap are made of easily floating materials that need to be weighted down or otherwise anchored to the subgrade prior to placement of the armour layer.

In addition, unless the work area is dewatered or isolated by a cofferdam, flow velocities greater than about 0.3 m/s can create large forces on the geotextile that often result in fabric wavelike undulations that are difficult to control. In mild currents, geotextiles are usually placed using a roller assembly, with sandbags to hold the fabric temporarily.

Blanket-like products consisting of two geotextiles with a layer of sand in between also exist. These stitch-bonded layers form a heavy, filtering geocomposite blanket that readily sinks. The composite geotextile has sufficient stability to be handled even when loaded by currents up to approximately 1 m/s (Heibaum, 2002).

In deep water or in currents greater than 1 m/s, sand-filled geotextile containers (sacks) underlying the armouring material can also be used (refer to Figure 5.5.4(a)). Geotextile containers combining the resistance against hydraulic loads with the required filtration capacity should be chosen (Heibaum, 2002). Geotextile containers have proven to give sufficient stability against erosive forces in many applications, including wave-attack environments.

Figure 5.5.4(a) – Schematic diagram showing sand filled geotextile containers as a filter

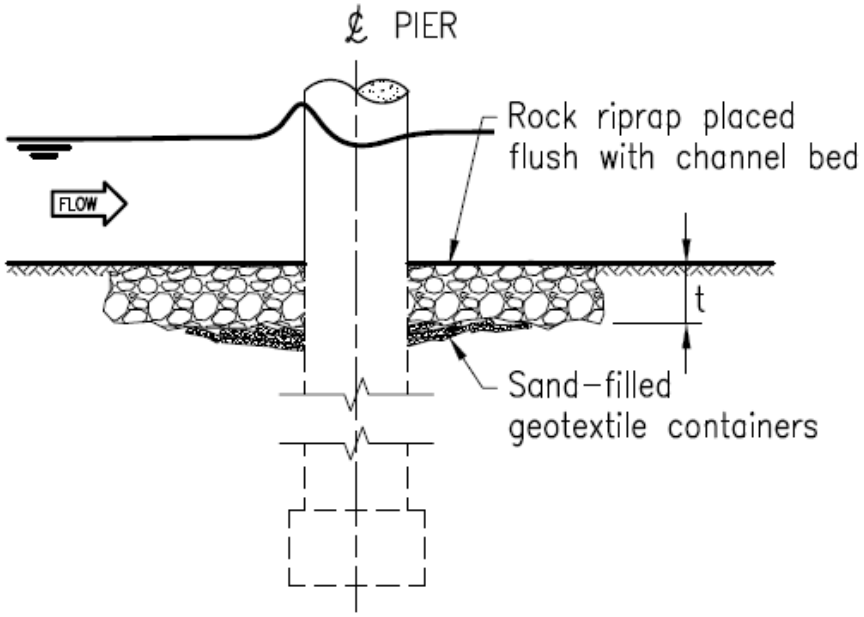

Rock riprap at bridge piers

Addition

The below four mechanisms of riprap failure at piers have been documented in several experimental studies:

- Shear failure, where the riprap stones are displaced by the flow, this occurs where the riprap is unable to resist the hydrodynamic forces induced by the flow.
- Winnowing failure, this occurs where the finer underlying bed material is eroded through riprap voids, this is more likely to occur in sandy bed rivers than in coarser bed materials. A filter is often recommended to avoid winnowing failure.
- Edge failure, refers to cases where the periphery of the riprap is undermined. Riprap is vulnerable to edge failure where there is insufficient lateral extent of the protective layer, and
- Bed-form undermining, where the riprap layer is undermined and settles away from the pier at the trough caused by large dunes.

The flow conditions under which different failure mechanisms occur are shown in Figure 5.5.4(b) in terms of zones of riprap stability. In this figure, U* is the bed shear velocity, U^*_{cs} is the critical bed shear velocity for the sediment size d, and U^*_{cr} is the critical bed shear velocity for the riprap of size d_r. The first three failure modes are observed in all flow conditions, while bed-form undermining only occurs under live-bed conditions. The likelihood of winnowing failure increases with U^*/U^*_{cs} , while edge failure is more likely at high U^*/U^*_{cr} values. Shear failure typically only occurs for U^*/U^*_{cs} >0.35. The diagram also shows that winnowing is more likely to occur for larger relative riprap sizes d_r/d (Melville and Coleman 2000).

Figure 5.5.4(b): Summary of pier riprap failure conditions for bed regimes

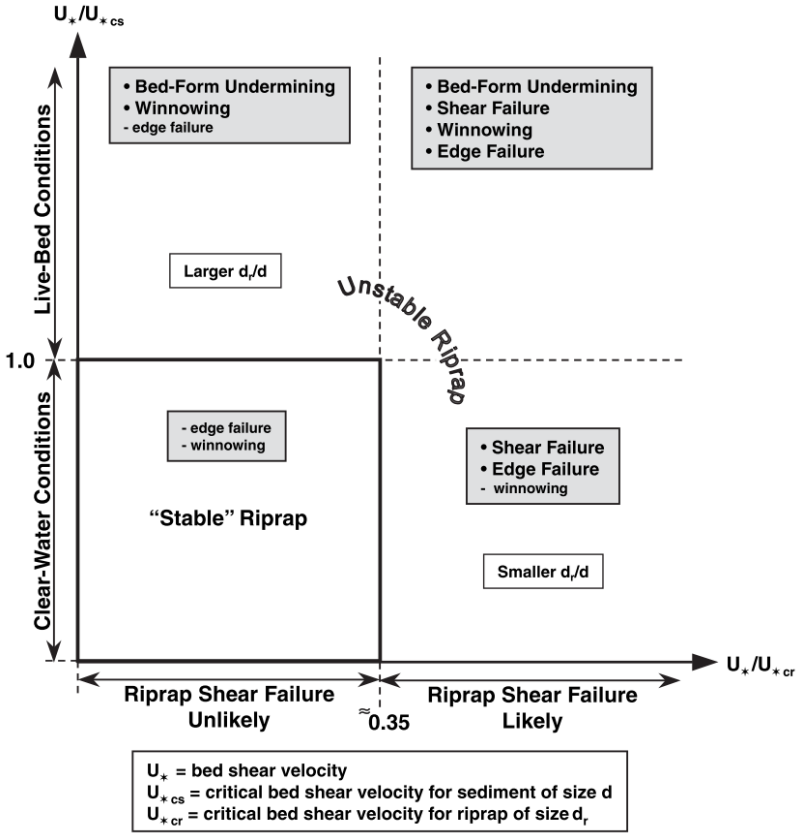

Source: modified from Lauchlan (1999)

The flow velocity approaching the piers can be estimated using factored average velocities at the cross section or velocities extracted directly from two-dimensional hydraulic modelling.

Rock-filled bags are other alternatives used to protect piers.

Mounding riprap around a pier is usually not acceptable because it obstructs flow, captures debris and increases scour potential at the periphery of the installation.

The riprap layer should have a minimum thickness (t) of two to three times the d_{50} of the rock (refer to Figure 5.5.4(c)), however, when the contraction scour at the bridge opening exceeds CFD_{50}, the riprap thickness must be increased to the full depth of adopted total scour depth to prevent undermining.

The lateral extent of protection surrounding the pier shall be at least two to three times the diameter of circular or octagonal piers, or, the width of rectangular pier columns, as appropriate. For wall piers or pile bents consisting of multiple columns where the axis of the structure is skewed to the flow, the lateral extent of the protection should be increased by a factor Kα (Richardson and Davis, 2001),

which is a function of the width (a) and length (L) of the pier (or pile bents) and the skew angle α as given below:

$$K_\alpha = \left(\frac{acos\alpha + Lsin\alpha}{a}\right)^{0.65}$$

A geotextile layer is typically required for riprap at bridge piers. The filter should not be extended fully beneath the riprap; instead, it should be terminated 2/3 of the distance from the pier to the edge of the riprap. The geotextile layer or a collar surrounding the pier should also be installed to protect the pier and prevent the leaching of the bed material from around the pier refer Figure 5.5.4(c).

If riprap is placed as scour protection around a pier, the bridge should be monitored and inspected during and after each high flow event to ensure that the riprap is stable.

Figure 5.5.4(c) - Riprap layout diagram for pier scour protection

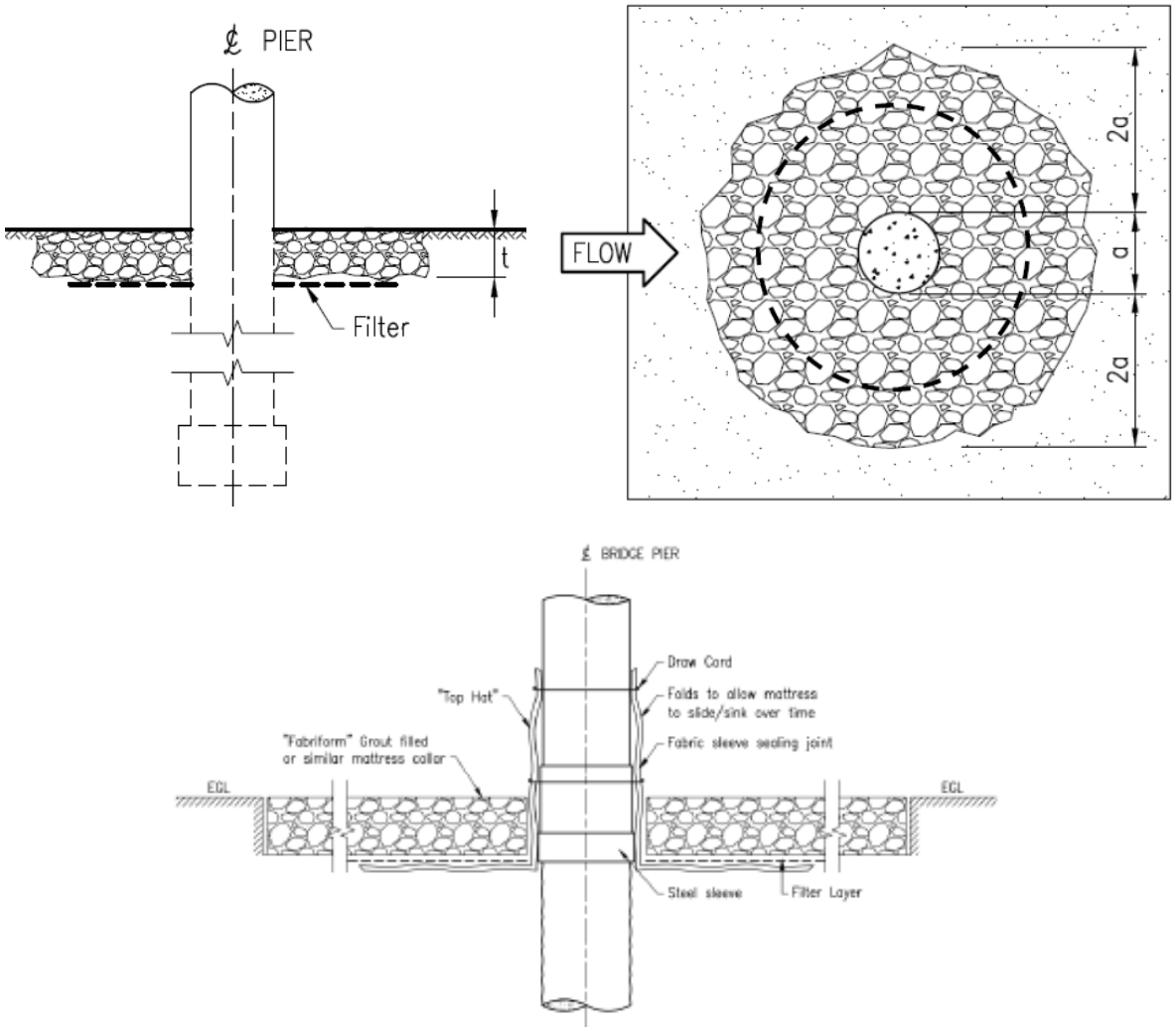

Sizing rock riprap at bridge piers

Other formulas can also be used to size riprap for bridge piers, Figure 5.5.4(d) compares the rearranged Isbash formula (Lagasse et al. 2009) with the Lauchlan (1999) method and an equation that fits the upper range of velocities for the rock classes recommended by one of the more widely used methods in Australia, the Austroads (1994) method (Melville and Coleman 2000). All plotted equations are listed in Table 5.5.4(a) in a common format to allow comparison.

The standard rock classes of riprap for different velocities recommended by the Austroads (1994) method are reproduced in Table 5.11 and Table 5.12 of Austroads (2018). These tables are based on the California Division of Highways (1970) equations with a slope of 1:1.5 and predict d_{33} (which leads to higher values if expressed in terms of the median riprap size, d_{50}). The original California Division of Highways (1970) equations are also included in Table 5.5.4(a) for reference.

Figure 5.5.4(d) shows that the Austroads (1994) method is heavily dependent on the velocity factor and generally leads to larger riprap sizes than both the Lauchlan (1990) method and the rearranged Isbash method (Lagasse et al. 2009).

Further, it must be noted that the California Division of Highways (1970) equation is heavily dependent on the gradient of the face slope. The Austroads (1994) method is based on the California Division of Highways (1970) equation with a 1:1.5 slope. A milder slope might be used within this equation at locations where the rock protection will be placed at milder slopes (for example at piers where the rock protection can be placed roughly following the bed stream slope).

Equation 5.5.4(e) fits the rock sizes (converted to d_{50}) obtained with the California Division of Highways (1970) equation using a milder 1:6 slope (more characteristic of rip rap placement at stream bed slopes).

Figure 5.5.4(d) shows that this equation predicts sizes smaller than those predicted by the Lagasse et al. (2009) and the Lauchlan (1999) equation roughly equating to sizes one class smaller than those recommended by the Austroads (1994) method (with a 1:1.5 slope). Based on Queensland experience, either the HEC-23 (preferred method in Austroads 2018) or the Transport and Main Roads (2019) equations are recommended. However, it should be noted that the Transport and Main Roads (2019) equation does not represent a mandatory Transport and Main Roads policy.

Figure 5.5.4(d) – Comparison of equations for sizing riprap at bridge piers

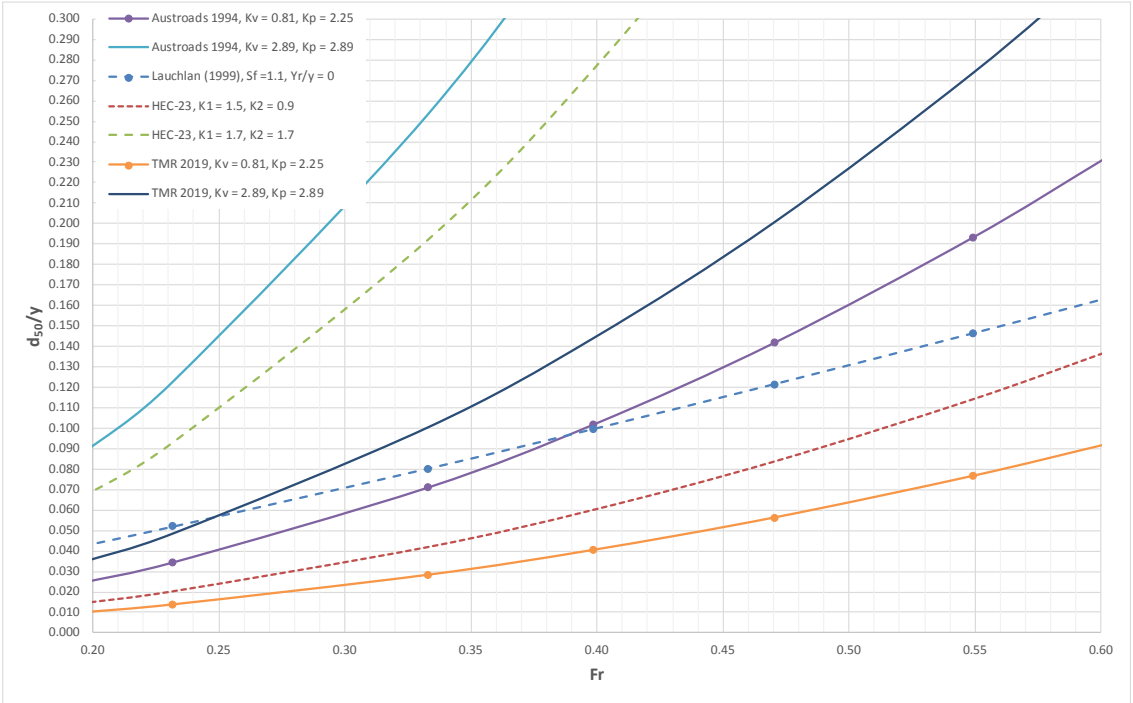

Table 5.5.4(a) – Equations for sizing riprap at bridge piers

Reference	Equation	Symbology
Austroads 1994*	$\frac{d_{50}}{y} = \frac{0.58 K_p K_v}{(S_s - 1)} Fr^2$ 5.5.4(a)	K_p, pier shape factor, 2.25 for round nose piers or 2.89 for rectangular piers and K_v, velocity factor, 0.81 for a pier near the bank of a straight channel to 2.89 for a pier at the outside bend of the main channel. F_r is the Froude number, Fr = $V_{max}/(gy)^{0.5}$, $_y$ water depth at the pier (m) and V_{max} is the maximum velocity at the channel (m/s).
HEC-23 (Lagasse et al. 2009)	$\frac{d_{50}}{y} = \frac{0.692(V_{des}^2) \cdot y}{(S_s - 1)2g}$ 5.5.4(b)	As recommended in Austroads, 2018.
Lauchlan 1999	$\frac{d_{50}}{y} = 0.3 S_f \left(1 - \frac{Y_r}{y}\right)^{2.75} Fr^{1.2}$ 5.5.4(c)	S_f is a safety factor with a minimum value recommended of 1.1. Y_r is the placement below bed level (m). Fr is the Froude number, Fr = $V_{max}/(gy)^{0.5}$, y water depth at the pier (m) and V_{max} is the maximum velocity at the channel (m/s).
California Division of Highways (1970)	$M_r = \frac{0.01135 V^6 S_s}{(S_s - 1)^3 sin^3(\rho - \sigma)}$ $\frac{d_{33}}{y} = \frac{0.274}{(S_s - 1) sin(\rho - \sigma)} Fr^2$ 5.5.4(d)	M_r mass(kg) of critical d_{33} stone, d_{33} stone size for which 33% are finer by weight, V mean velocity adjacent to riprap, α = embankment slope (º), ρ = 70º for randomly placed rubble and broken rock. Fr is the Froude number, Fr = $V_{max}/(gy)^{0.5}$, y water depth at the pier (m) and V_{max} is the maximum velocity at the channel (m/s).
Transport and Main Roads 2019**	$\frac{d_{50}}{y} = \frac{0.23 K_p K_v}{(S_s - 1)} Fr^2$ 5.5.4(e)	K_p, pier shape factor, 2.25 for round nose piers or 2.89 for rectangular piers and K_v, velocity factor, 0.81 for a pier near the bank of a straight channel to 2.89 for a pier at the outside bend of the main channel. Fr is the Froude number, Fr = $V_{max}/(gy)^{0.5}$, y water depth at the pier (m) and V_{max} is the maximum velocity at the channel (m/s).

*Equation 5.5.4(a) developed by Melville and Coleman (2000), fits the upper range of velocities of the rock classes recommended by the Austroads (1994) method. ** Equation 5.5.4(e) fits the rock sizes obtained using Equation 5.4.4(d) with a 1:10 slope and converted to obtain (d_{50}).

Rock riprap at abutments

The minimum riprap layer thickness (t) recommended for the different rock classes is listed in Table 5.11 (Austroads, 2018), this equates to at least two layers of the selected rock class or 1.7 to 2 d_{50}.This thickness might be increased by 50% if placed under water to provide for the uncertainties associated with this type of placement.

It should also be noted that the standard sizes shown in Table 5.12 (Austroads, 2018) are defined as percentage of rock larger (heavier) than, while all presented equations and most sizing methods define the sizes inversely (that is, as percentage of rock finer / lighter than).

HEC-23 (Lagasse et al. 2009) presents an alternative gradation to that recommended in (Austroads, 2018). This gradation reproduced in Table 5.5.4(b) (in SI units) recommends 10 different classes instead of seven. This criterion is based on a nominal or "target" d_{50} and a uniformity ratio d_{85}/d_{15} that results in well graded riprap. The target uniformity ratio d_{85}/d_{15} is 2.0 with an allowable range from 1.5 to 2.5.

A minimum d_{50} for the riprap might be specified, thus indicating the size for which 50% of the particles are smaller. Stone sizes can also be specified in terms of weight (e.g., W_{50}) using an accepted relationship between size and volume and a known (or assumed) rock density.

Table 5.5.4(c) provides the equivalent particle weights for the ten rock classes, assuming the volume of stone is 85% of a cube and using a specific gravity of 2.65 for the rock density.

It should be noted that quarries in Queensland might not have readily available any of the rock classes recommended either by either Austroads (1994) or Lagasse et al. (2009). When this is the case, either the specifications can be provided to the quarry for rock to be purposely crushed or available rock sizes with the closest equivalent characteristics should be used. In some cases, the use of precast concrete interlocking armour elements might also be considered.

Spill-through abutment slopes should be protected with the selected rock riprap size to a minimum elevation of 0.6 m above the water elevation expected for ULS conditions. If the bridge is overtopped during ULS conditions, the entire abutment should be protected.

A self-launching apron surrounding the abutment should also be provided to protect the toe of the abutment, the length of this apron shall extend from the toe of the abutment into the bridge waterway a minimum distance of twice the flow depth in the overbank area near the embankment but should not exceed 7.5 m (Atayee et al. 1993). Transport and Main Roads abutment protection standard drawings 2232 to 2237 depict examples of aprons suitable for cases with low scour depths. For cases with large scour depths, the apron length and/or thickness shall be designed to protect the edge of the abutment from adopted scour depths (Lagasse et al. 2009). Melville and Coleman (2000) recommend sizing the apron length based on the adopted scour depth at the abutment (Y_s) and the angle of repose (θ) of the launched riprap after scour ($L_{apron} = Tan\theta * Y_s$).

The top surface of the apron should be flush with the existing grade of the floodplain, as the riprap layer can block a significant portion of the bridge conveyance area and could generate significant scour around the apron (refer to Figure 5.5.4(e)). The apron should wrap around the abutment to at least the tangent point with the roadway embankment slopes, however additional protection might be required beyond this point for overtopping bridges. Lagasse et al. (2009) recommend extending the length of the downstream embankment protection by 2 flow depths or 7.5 m, whichever is larger, to protect the roadway embankment (refer to Figure 5.5.4(e)). However, for overtopping bridges the upstream face of the roadway embankment might also be extended.

Ultimately, engineering judgement by an experienced Registered Professional Engineer of Queensland (RPEQ) should be exercised to design riprap countermeasures for abutments.

Table 5.5.4(b) – Minimum and maximum allowable particle size (HEC-23, Lagasse et al. 2009)

Nominal riprap class by median particle diameter		**d_{15}**		**d_{50}**		**d_{85}**		**d_{100}**
Class	Size (m)	Min	Max	Min	Max	Min	Max	Max
I	0.15	0.094	0.132	0.145	0.175	0.198	0.234	0.305
II	0.25	0.140	0.198	0.216	0.267	0.292	0.356	0.457
III	0.30	0.185	0.267	0.292	0.356	0.394	0.470	0.610
IV	0.40	0.234	0.330	0.368	0.445	0.495	0.584	0.762
V	0.50	0.279	0.394	0.432	0.521	0.597	0.699	0.914
VI	0.55	0.330	0.470	0.508	0.610	0.699	0.826	1.067
VII	0.65	0.368	0.533	0.584	0.699	0.787	0.940	1.219
VIII	0.8	0.470	0.660	0.724	0.876	0.991	1.168	1.524
IX	1	0.559	0.800	0.864	1.054	1.194	1.410	1.829
X	1.1	0.648	0.927	1.016	1.232	1.384	1.638	2.134

Table originally published in imperial units, *Particle size d corresponds to the intermediate axis of the particle.

Table 5.5.4(c) – Minimum and maximum allowable particle weight (HEC-23, Lagasse et al. 2009)

Nominal riprap class by median particle weight		**W_{15}**		**W_{50}**		**W_{85}**		**W_{100}**
Class	Weight	Min	Max	Min	Max	Min	Max	Max
I	9 kg	2	5	7	12	18	29	64
II	32 kg	6	18	23	43	56	101	215
III	80 kg	14	43	56	101	137	234	510
IV	150 kg	29	81	113	198	274	449	997
V	1/4 tonne	49	137	181	318	479	768	1722
VI	3/8 tonne	81	234	295	510	768	1267	2735
VII	1/2 tonne	113	342	449	768	1100	1870	4082
VIII	1 tonne	234	649	854	1516	2190	3593	7973
IX	2 tonnes	393	1154	1451	2638	3832	6310	13777
X	3 tonnes	612	1795	2362	4211	5975	9905	21878

Table originally published in imperial units, for rock sizing purposes an imperial ton and a metric ton can be assumed to be equivalent.

Figure 5.5.4(e) – Extent of riprap apron at abutments (after Lagasse et al. 2009)

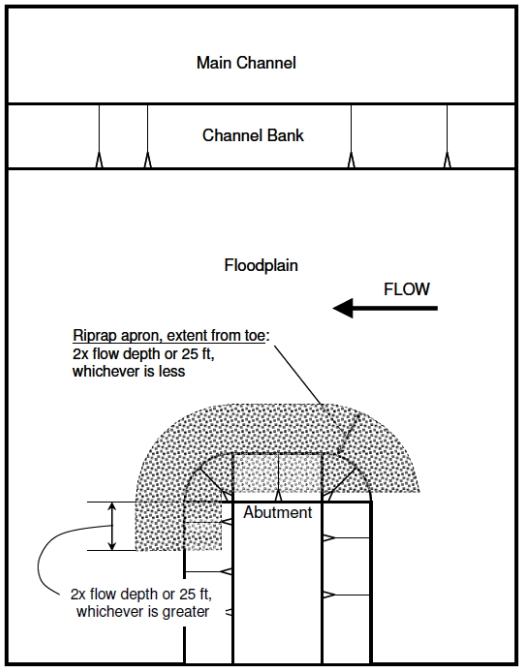

a) Plan

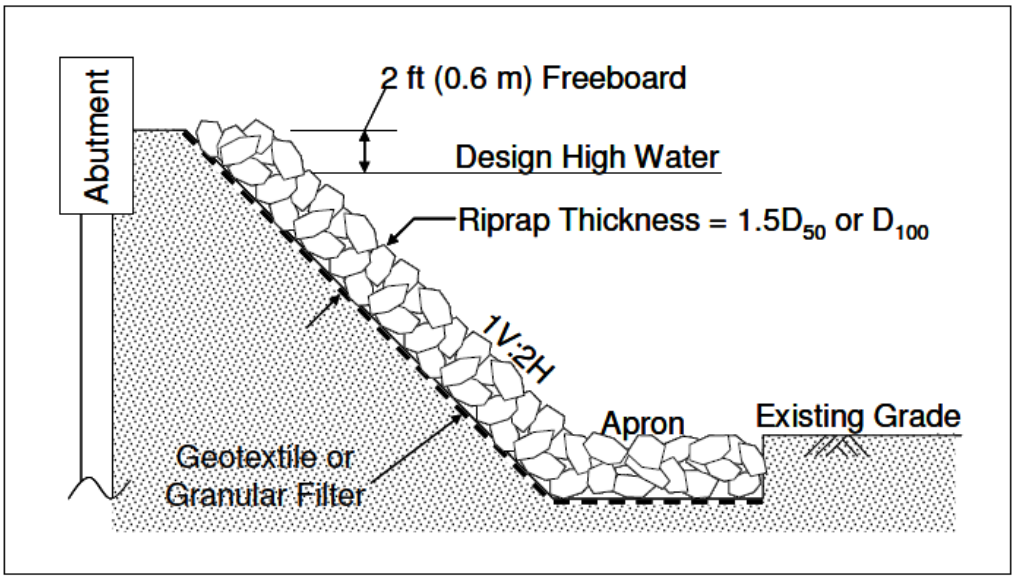

b) Section

Sizing rock riprap at abutments

Similarly to piers, other formulas can be used to size riprap for bridge abutments.

Table 5.5.4(d) and Figure 5.5.4(f) compare some of the most commonly used formulas with the Richardson and Davis (1995) method recommended in Austroads (2018).

Figure 5.5.4(d) shows that the Croad (1989) and Pagan-ortiz (1991) methods lead to larger riprap sizes than both the Austroads (1994) and Richardson and Davis (1995) method (Lagasse et al. 2009 and Austroads 2018). Melville et al. (2007) recommends the use of either of the Richardson and

Davies (1995) or Pagan-Ortiz (1991) equations along with appropriate factors of safety for design purposes.

Based on Queensland experience, either the Austroads (1994) or the Richardson and Davis (1995) methods are recommended.

When the velocities at the abutment can be accurately identified (i.e. based on two-dimensional model results), the highest value of the maximum velocities observed at the cross section and the factored average cross section velocities might also be used within the below methods.

However, it should be noted that two-dimensional model derived velocities can be misleading at very shallow depths, as large velocities might be artificially caused by model instabilities. Validation using other methods and engineering judgement should be used when unrealistically large velocities are observed at bridges.

Note that while riprap size is appropriately selected based on stability against shear and edge failure, the possibility of winnowing or bed-form undermining should be considered in design.

Figure 5.5.4(f) – Comparison of equations for sizing riprap at abutments

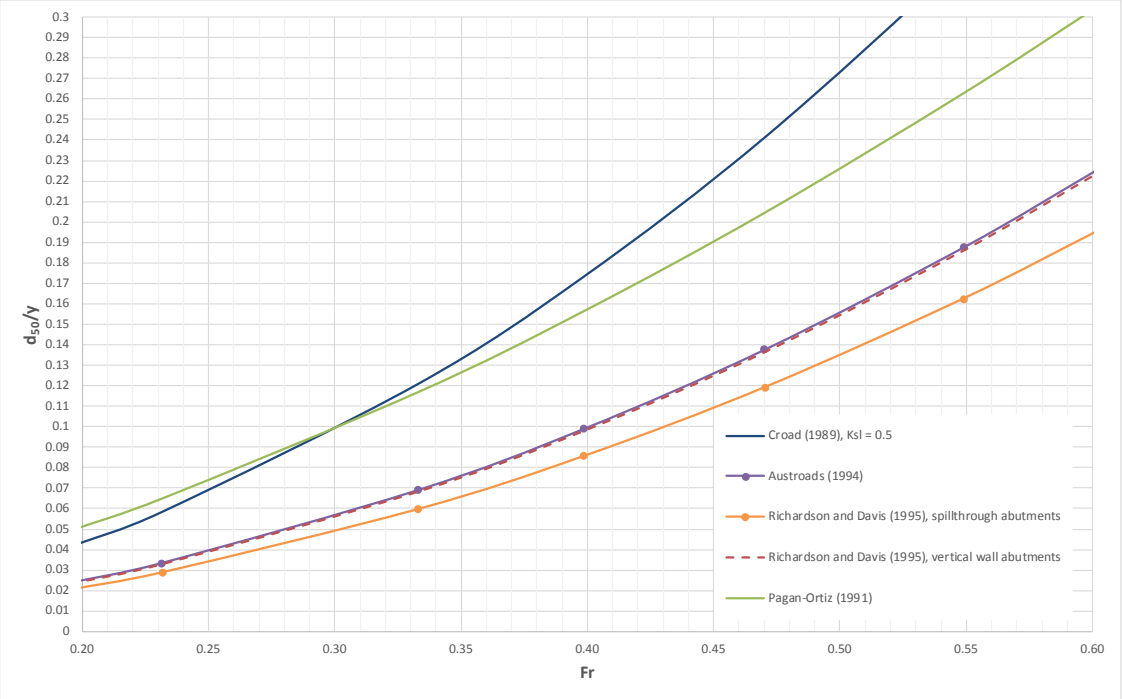

Among other countermeasures, HEC-23 (Lagasse et al. 2009) include detailed design guidelines for grout filled mattresses, guide banks and spurs. Rigid grout filled mattresses require careful design to avoid undermining when used as abutment protection, however they are not recommended at bridges that experience average stream velocities higher than 2 m/s.

Gravity wall systems comprising large, permeable, interlocked, precast concrete blocks have been recently used by Transport and Main Roads for various scour remediation applications (refer to Figure 5.32 in Austroads, 2018). One of the main advantages of these precast systems is the ability to be rapidly constructed, especially as part of flood recovery works. The blocks can be manufactured off-site and are ideal especially in areas where local sources of large sound rock are not available. The system has a limited flexibility to move compared to a rigid system.

Sizing is similar to classes of rock determined from Table 5.11 in Austroads, 2018 with different sizes and weight of units approximately equivalent to ½ tonne, 1 tonne or 2 tonne riprap classes. It should

be noted that the use of these measures requires hydraulic, structural and geotechnical design to ensure their stability.

Table 5.5.4(d) – Equations for sizing riprap at bridge abutments

Reference	Equation	Symbology
Austroads 1994*	$\frac{d_{50}}{y} = \frac{1.026}{(S_s - 1)} Fr^2$ 5.5.4(f)	Fr is calculated using the average bridge velocity factored by V= 1.33*V_{avg}, as recommended in Austroads (1994). Non-factored maximum velocity at the cross section might also be used within this formula.
Richardson and Davis (1995)	$\frac{d_{50}}{y} = \frac{K_s}{(S_s - 1)} Fr^2 \quad Fr \leq 0.8$ $\frac{d_{50}}{y} = \frac{K_s}{(S_s - 1)} Fr^{0.28} \quad Fr > 0.8$ 5.5.4(g)	Shape factor K_s = 0.89 for spill through abutments and 1.02 for vertical wall abutments for Fr<=0.8, for Fr > 0.8 K_s = 0.61 for spill through abutments and 0.69 for vertical wall abutments. Fr is calculated using the average bridge velocity, S_s specific gravity of rock (2.65), y depth of flow in the contracted bridge opening, g is the gravitational acceleration. This is the preferred method in Austroads (2018).
Croad (1989)	$\frac{d_{50}}{y} = 0.025 V_b^2 K_{sl}^{-1}$ $K_{sl} = \sqrt{1 - \frac{sin^2 \propto}{sin^2 \theta}}$ 5.5.4(h)	V_b = velocity at abutment = 1.5*V_{avg}, K_{sl} is the embankment slope factor, α = slope angle, θ = angle of repose. Note that typical abutments have a slope of 1:1.5 (α = 33.69). A typical angle of repose for angular riprap is θ = 40. Non-factored maximum velocity at the cross section might also be used with this formula.
Pagan-Ortiz (1991)	$d_{50} = \left(\frac{1.064 V^2 y^{0.23}}{(S_s - 1) g}\right)^{0.81}$ 5.5.4(i)	V is the average velocity in the contracted bridge opening, S_s specific gravity of rock (2.65), y depth of flow in the contracted bridge opening, g is the gravitational acceleration.

5.6 Monitoring bridges for scour

Difference

For existing state-controlled road bridges in Queensland, monitoring of bed level is undertaken in accordance with Transport and Main Roads *Structures Inspection Manual* (TMR, 2016). Bed levels (soundings) at each pier and abutment are routinely measured during Transport and Main Roads Level 2 and 3 bridge inspections. Additional bed levels are also undertaken after a bridge has been overtopped or for some bridges located immediately downstream of dams, which are monitored after every rain event, irrespective of whether they are overtopped.

While this method does not record the maximum depth of scour during a flood, this is not critical for most of the bridges.

Bridge inspection reports enclose all information collected during inspection, based on this data the Bridge Asset Management unit at Transport and Main Roads calculates critical scour depths for piers and abutments at all bridges. This information provides an invaluable insight of the history of scour at the structure and should be considered during bridge upgrades or for scour remediation at existing bridges.

The bed profile at the bridge at each pier and abutment should be surveyed at the time of construction. This information provides the reference information to monitor long-term trends in the stream bed profile (contraction scour) and detect any changes in bed depth at piers and abutments (local scour). The current bed level should always be compared to the design level.

For some bridges, permanent scour monitoring may be required. Use of fixed or discrete scour monitoring instrumentation has proved to be more effective than visual inspections. Various techniques used to monitor the scour in 'real time' are discussed below. The use of these devices enables long-term monitoring to determine long-term trends. They also provide information on bed movements in flood.

Addition

Instruments to monitor bridge scour can be divided into portable and fixed types. The use of fixed or portable instruments to monitor scour depends on many different factors as each instrument has advantages and limitations that influence when and where they should be used.

Fixed instrumentation is normally used when frequent measurements or regular, ongoing monitoring are required. Portable instruments are preferred when only occasional measurements are required, or when many different bridges must be monitored on a relatively infrequent basis.

The frequency of data collection desired, the physical conditions at the bridge and stream (such as height off the water and type of superstructure), and traffic safety issues can influence the decision to use fixed or portable equipment. Ultimately, the selection of any type of instrumentation must be based on a clear understanding of its advantages and limitations, and in consideration of the conditions that exist at the bridge and in the waterway. Some of the most commonly used portable and fixed scour measuring instruments are listed in Table 5.6 alongside their advantages and limitations.

Chapter 9 of HEC-23 (Lagasse et al. 2009) includes a comprehensive description of the most common scour monitoring and instrumentation methods while Prendergast and Gavin (2014) discuss recent advances on monitoring methods based on the dynamic response of a bridge to scour.

Table 5.6 – Summary of Scour monitoring instrumentation (adapted from Lagasse et al., 2009)

Type	Best Application	Advantages	Limitations
Portable systems			
Portable physical probes	Small bridges and streams	Simple technology.	Accuracy, high flow application.
Portable sonar	Larger bridges and streams	Point data or complete mapping, accurate.	High flow application.
GPR	Forensic evaluation	Accurate depth-structure of stream channel and under water bottom sediment layers.	High cost, complex equipment and data analysis, calibration data required. Does not work in dense clay soils, saltwater conditions or deep channels (> 9 m).
Survey	Small, shallow channels	Common technique.	Not possible during flood events or at deep channels.
Fixed systems			
Sonar	Coastal regions, deep wide navigational channels	Records infilling, time history, can be built with off the shelf components.	Debris, high sediment loading, ice and air entrainment can interfere with readings. Battery life.
Magnetic sliding collar / scubamouse	Fine bed channels	Simple, mechanical device.	Vulnerable to ice and debris impact; only measures maximum scour; unsupported length, binding.
Tiltmeter arrays	All	May be installed on the bridge structure and not in the stream-bed and/or underwater.	Provides bridge movement data which may or may not be related to scour.
Float-out device	Ephemeral channels	Lower cost, ease of installation, buried portions are low maintenance and not affected by debris, ice or vandalism.	Does not provide continuous monitoring of scour; battery life.
Sounding rods	Coarse bed channels	simple, mechanical device.	Unsupported length, binding, augering.
TDR	Riverine ice channels	robust, resistance to ice, debris and high flows.	Limit on maximum lengths for signal reliability of both cable and scour probe, Battery life.

5.6.1 Sonar scour monitor

Addition

Current monitors range from fish finders to smart sonar transducers, both of which are commercially available. These instruments can track both the scour and deposition processes (Lagasse et al. 2009).

5.6.2 Magnetic sliding collar monitor

Addition

Magnetic sliding collar monitors and 'Scubamouse' devices both work on the principle of a manual or automated gravity-based physical probe that rests on the streambed and moves downward as scour develops.

The 'Scubamouse' consists of a vertical steel rod buried or driven into the streambed in front of the bridge pier around which is placed a horseshoe-shaped radioactive collar that initially rests on the streambed. The collar slides down the pipe and sinks to the bottom of the scour hole as scour progresses during a flood (see Figure 5.6.2(a)). The position of the collar is determined by sending a radiation detector down the rod after the flood. This device has been installed on some bridges in New Zealand (Melville et al. 1989).

Figure 5.6.2(a) – Scubamouse at Waikato River Bridge at Tuakau

(Photo courtesy of Bruce Melville).

5.6.3 Float-out devices

Addition

These devices are particularly easy to install in dry riverbeds, during the installation of an armouring countermeasure such as riprap, and during the construction of a new bridge (Lagasse et al. 2009).

5.6.4 Sounding rods

Addition

Sounding rods can be either portable or fixed instruments. Portable rods refer to any type of device that extends beyond the reach of the inspector, the most common being sounding poles and sounding weights (or lead lines) which are typically a torpedo shaped weight suspended by a measurement

cable. Portable rods can be used from the bridge or from a boat or by a diver. Fixed sounding rods are permanently attached to bridge piers.

Physical probes only collect discrete data (not a continuous profile), and can be limited by large depth and velocity (e.g. during flood flow condition) or debris accumulation. Advantages of physical probing include not being affected by air entrainment or high sediment loads, and it can be effective in shallow water.

5.6.5 Time Domain Reflectometry (TDR)

Accepted

5.6.6 Ground-Penetrating Radar (GPR)

Accepted

5.6.7 Tiltmeter arrays

Accepted

5.6.8 Operational considerations

Addition

In practical applications, particularly under flood flow conditions, the inability to properly position any portable measuring instrument often limits the accuracy of the measurements. Portable (non- floating and floating) instruments can be deployed from the bridge deck or from the water surface.

Non-floating systems generally involve standard stream gauging equipment and procedures, including the use of sounding weights (or rods with the scour measurement device attached to the end). Note that these hand-held probes are not generally useable during flood flow conditions.

Float based systems permit measurement beneath the bridge and alongside the bridge piers. Floats are a low-cost approach that have been used with some success during flood flow conditions. A variety of float designs have been proposed and used to varying degrees for scour measurements, typically to deploy a sonar transducer. Common designs include foam boards, PVC pontoon configurations, spherical floats, water skis and kneeboards (Lagasse et al. 2009). The size of the float is important to stability in fast moving, turbulent water.

Water surface deployment typically involves a manned boat, however, safety issues under flood conditions have suggested the use of unmanned vessels.

References

Australian Standard, AS 5100.1-2017, *Bridge design: Part 1: Scope and general principles.*

Australian Standard, AS 5100.2-2017, *Bridge design: Part 2: Design loads.*

Ashmore, P. and Parker, G. (1983), *Confluence Scour in coarse braided streams,* Water Resources Research, 19(2), 392-402.

Arneson L.A. Zevenbergen L.W. Lagasse P.F., Clopper P.E. (2012), *Evaluating Scour at bridges, 5th Edition, Hydraulic Engineering Circular No.18, Publication No. FHWA-HIF-12-003*, U.S. Department of Transportation, Federal Highway Administration, Colorado, U.S.A.

Austroads (1994), *A Guide to the Hydraulic Design of Bridges, Culverts and Floodways*, Flavell D. Technical Editor, Sydney, NSW, Australia.

Austroads (2018), *Guide to Bridge Technology Part 8: Hydraulic Design of Waterway Structures*, prepared by Hanson Ngo, Project Managers: Phanta Khamphounvong and Henry Luczak, Sydney, NSW, Australia.

Blench T. (1969), *Mobile-bed Fluviology*, University of Alberta Press, Edmonton, Canada.

Briaud J.L., Chen H. C., Chang K.A., Oh S.J, Chen S., Wang J., Li Y.,Kwak K., Nartajho P., Gudaralli R., Wei W., Pergu S., Cao Y.W. and Ting F. (2011), *The SRICOS-EFA Method*, Texas A&M University, U.S.A.

California Division of Highways (1970), *Bank and Shore Protection in California Highway Practice*, Sacramento, California, U.S.A.

Croad, R.N. (1989), *Investigation of the pre-excavation of the abutment scour hole at bridge abutments*, Report 89-A9303, Central laboratories, Works and Development Services Corporation (NZ) LTD, Lower Hutt, New Zealand.

Ettema R., Constantinescu G. and Melville B.W (2017), *Flow-Field Complexity and Design Estimation of Pier-Scour Depth: Sixty Years since Laursen and Toch*, Journal of Hydraulic Engineering, ASCE 143(9) September 2017.

Federal Highway Administration, 2012c, *Submerged-Flow Bridge Scour under Clear-Water Condition*, Federal Highway Administration, Report No. FHWA-HRT-12-034 (Suaznabar, O., H. Shan, Xie, Z., Shen, J., and Kerenyi, K.).

Florida Department of Transport, FDOT, (2011), *Bridge Scour Manual*, Tallahassee, Florida, U.S.A.

Heibaum, M.H., (2002), *Geotechnical Parameters of Scouring and Scour Counter-measures*, Mitteilungsblatt der Bundesanstalt für Wasserbau Nr. 85. (J. Federal Waterways Engineering and Research Institute, No. 85), Karlsruhe, Germany.

Kirby, A.M., Roca M., Kitchen A., Escarameia, M.and Chesterton, O.J. (2015), *Manual on Scour at bridges and Other Hydraulic Structures*, 2nd Edition, CIRIA, London, U.K.

Klaasen, G.J and Vermeer, K. (1988), *Confluence Scour in large braided rivers with fine bed material*, Proc. International Conf. on Fluvial Hydraulics, Budapest, Hungary, 395-408.

Lacey, G. (1930), *Stable Channels in Alluvium,* paper 4736, Minutes of the proc*.,* Institution of Civil Engineers, Vol. 229, William Cloves and Sons Ltd., London, UK, 259-292.

Lagasse, P.F, Clopper P.E., Pagán-Ortiz J.E., Zevenbergen L.W.,. Arneson L.A, Schall J.D., and Girard L.G. (2009), *Bridge Scour and Stream Instability Countermeasures - Experience, Selection, and Design Guidelines*, Hydraulic Engineering Circular No. 23, Third Edition, FHWA-NHI 09-111 (Vol. 1), FHWA-NHI-09-112 (Vol. 2), Federal Highway Administration, Washington, D.C.

Lauchlan, C.S. (1999), *Countermeasures for Pier scour*, PhD Thesis, The University of Auckland, Auckland, New Zealand.

Lyn, D.A. (2008), *Pressure Flow Scour: A Re-examination of the HEC-18 Equation*, Journal of Hydraulic Engineering, ASCE, Vol. 134, No. 7, July. 2008, Pag 1015-1020.

Maynord, S.T. (1996), *Toe-scour estimation in stabilised bendways*. Journal of Hydraulic Engineering ASCE, 122(8), 460-464.

Melville, B. W. and Coleman, S. E. (2000), *Bridge Scour*, Water Resources Publications, LLC, Colorado, U.S.A.

Melville, B. W., Van Ballegooy, S, Coleman, S. E. and Barkdoll, B. (2007), *Riprap Size Selection at Wing-wall Abutments*, Journal of Hydraulic Engineering, ASCE, Vol. 133, No. 11, Nov. 2007, Pag. 1265-1269.

Melville B.W. (2014), *Pressure Flow Scour at Bridges*, Scour and Erosion Proceedings of the 7th International Conference on Scour and Erosion, Perth, Australia, 2-4 December 2014.

Moreno, M., Maia, R., Couto, L., and Cardoso, A. (2016a), *Prediction of equilibrium local scour depth at complex bridge piers,* J. Hydraul. Eng. ASCE, 10.1061/(ASCE).

National Cooperative Highway Research Program, (2010), *Estimation of Scour Depth at Bridge Abutments, NCHRP Project 24-20, Draft Final Report*, Transportation Research Board, National Academy of Science, Washington, D.C., U.S.A, (Ettema, R., Nakato, T., and Muste, M.).

National Cooperative Highway Research Program, NCHRP. (2011a), *Evaluation of Bridge Pier Scour Research: Scour Processes and Prediction, NCHRP Project 24-27(01)*, Transportation Research Board, National Academy of Science, Washington, D.C. (Ettema, R., Constantinescu, G., and B.W. Melville).

National Cooperative Highway Research Program. (2011c), *Scour at Wide Piers and Long Skewed Piers, NCHRP Report 682*, Transportation Research Board, National Academy of Science, Washington, D.C., (Sheppard, D.M., Melville, B.W., and Deamir, H.).

Neill C.R. (1973), *Guide to Bridge Hydraulics*, Roads and Transportation Association of Canada, University of Toronto Press, Toronto, Canada.

Prendergast and Gavin. (2014), *A Review of Bridge Scour Monitoring Techniques*, Journal of Rock Mechanics and Geotechnical Engineering 6(2014) 138-149.

Pagán-Ortiz, J.E. (1991), *Stability of rock riprap for protection at the toe of abutments located at the floodplain*, FHWA-RD-91-057, Federal Highway Administration, Washington, DC, U.S.A.

Queensland Department of Transport and Main Roads, (TMR 2016), *Structures Inspection Manual.*

Queensland Department of Transport and Main Roads, (TMR 2018a), *Design Criteria for Bridges and Other Structures.*

Queensland Department of Transport and Main Roads, (TMR 2018b), MRTS03 *Drainage, Retaining Structures and Protective Treatments,* Technical Specification.

Queensland Department of Transport and Main Roads, (TMR 2018c), *North Kariboe Creek Bridge Replacement – Detailed Design – Hydraulic Analysis Report.*

Raudkivi A. J. and Melville B.W. (1996), *Effects of Foundation Geometry on bridge Pier Scour*, Journal of Hydraulic Engineering ASCE,122(4).

Richardson, E.V. and Davis, S.R. (2001), *Evaluating scour at bridges: Fourth edition, HEC-18, FHWA-NHI 01-001*, United States Department of Transportation, Washington, D.C.

Saynor, M.J., Erskine, W., and Lowry, J. (2008), Report: Geomorphology. In Lukacs G.P. and Finlayson C.M. (eds). *A compendium of Ecological Information on Northern tropical rivers. Sub-project 1 of Australia's Tropical Rivers – An integrated data assessment in Analysis (DET18). A report to Land and Water, Australia. National Centre for Tropical Wetland Research*, Townsville, Queensland, Australia.

Sheppard, D.M. and Miller, W. (2006), *Live-bed Local Pier Scour Experiments*, Journal of Hydraulic Engineering - ASCE, 132(7), 635-642.

Sheppard, D. M., Demir, H., and Melville, B. (2011), *Scour at wide piers and long skewed piers*. National Cooperative Highway Research Program Rep. 682, Transportation Research Board, Washington, D.C, U.S.A.

SMEC (2016), *Dawson Highway: Timber Bridges Replacement Project Preliminary and Detailed Design, 100% Design – BR05 – Doubtful Creek Bridge*. Prepared for Department of Transport and Main Roads, Fitzroy Region.

Transportation Research Board (TRB), (1994), *Scour Around Wide Piers in Shallow Water,* TRB Record 1471, Transportation Research Board, Washington, D.C. (Johnson, P.A. and Torrico E.F.).

Transportation Research Board (TRB), (1998), *Vertical contraction scour at bridges with water flowing under pressure conditions*. Transportation Research Board, Washington, D.C., TRB Record. 1647, 10-17 (Arneson, L.A. and S.R. Abt).

Umbrell, E.R., Young, G.K., Stein, S.M., and Jones, J.S., (1998), *Clear-water contraction scour under bridges in pressure flow*. J. Hydraul. Engrg. 124(2), 236-240.

Witheridge G.(2017a), *Erosion & Sediment Control Field Guide for Road Construction – Part 1*. Catchments and Creeks Pty Ltd., Brisbane, Queensland, Australia.

Witheridge G.(2017b), *Erosion & Sediment Control Field Guide for Road Construction – Part 2*. Catchments and Creeks Pty Ltd., Brisbane, Queensland, Australia.

Yang Y., Melville, B.W., Sheppard, A.M. and Shamseldin A.Y. (2018), *Clear-water Local scour at Skewed Complex Bridge Piers*, Journal of Hydraulic Engineering, ASCE, Vol. 144, No. 6.